

# HEC MONTRÉAL

## A Benders Decomposition Algorithm for the Maximum Availability Service Facility Location Problem

Par

Ali Muffak

Directeur de recherche

Okan Arslan, Ph.D.

Sciences de la gestion

(Analytique d'affaires)

*Mémoire présenté en vue de l'obtention  
du grade de maîtrise ès sciences en gestion  
(M. Sc.)*

Avril 2021

© Ali Muffak, 2021



# Résumé

Ce document présente le “*maximum availability service facility location problem*” (MASFLP). Le MASFLP vise à localiser des installations de service public autour de clients stationnaires à leur origine, à leur destination, ou sur leur chemin de l’origine à la destination (OD). Chaque client a accès au service durant son temps disponible, pendant une durée maximale, afin de respecter l’équité dans l’offre du service entre les différents clients. Nous présentons une formulation de programmation linéaire en nombres entiers mixte pour le MASFLP et nous développons un algorithme basé sur la décomposition de Benders pour résoudre le problème de manière analytique. Nous menons des expériences informatiques approfondies et rapportons les résultats de quatre techniques d’accélération différentes, notamment la génération de coupes multiples et des coupes Pareto-optimales. Notre algorithme fait mieux que CPLEX sur des petits et moyens problèmes et résout les grands problèmes allant jusqu’à 1000 noeuds, 1 million de paires OD et 100 installations de service. Nous menons également une étude de cas avec des données réelles de la ville de Chicago et montrons des applications de notre modèle en situation de pandémie. Nous montrons que les restrictions de confinement n’affectent pas la couverture et que l’optimisation des installations est plus efficace lorsque les restrictions sont prises en compte.

*Mots clés:* optimisation de l’emplacement, installations de service, décomposition de Benders, coupe Pareto-optimale

## Table des Matières

<b>Résumé</b>	<b>iii</b>
<b>Avant-propos</b>	<b>vii</b>
<b>Remerciements</b>	<b>viii</b>
<b>Chapitre 1: Introduction</b>	<b>2</b>
<b>Chapitre 2: Article</b>	<b>8</b>
<b>1 Introduction</b>	<b>8</b>
<b>2 Mathematical model</b>	<b>12</b>
2.1 Problem definition and notation . . . . .	12
2.2 Mathematical model . . . . .	14
<b>3 Benders Decomposition</b>	<b>14</b>
3.1 Benders subproblem . . . . .	15
3.2 Benders master problem . . . . .	16
3.3 Subproblem solution . . . . .	16
3.4 Benders cut selection scheme 1: single-cut . . . . .	19
3.5 Benders cut selection scheme 2: multi-cut . . . . .	19
3.6 Benders cut selection scheme 3: Pareto-optimal cut . . . . .	19
3.7 Magnanti-Wong problem solution . . . . .	20
<b>4 Computational Study</b>	<b>21</b>
4.1 Design of Experiments . . . . .	21
4.2 Computational Results . . . . .	22
<b>5 Chicago Case Study</b>	<b>27</b>
5.1 Computational Performance . . . . .	28
5.2 Discussion . . . . .	29
<b>6 Conclusion</b>	<b>37</b>
<b>References</b>	<b>38</b>

<b>Chapitre 3: Conclusion</b>	<b>40</b>
<b>Bibliographie</b>	<b>42</b>

## Liste des tableaux

1	Comparison of BD subproblem solved analytically and subproblem solved using LPs. . . . .	23
2	Performance comparison of the BD algorithms and CPLEX on small instances. 25	
3	Summary of computational results on small instances. . . . .	26
4	Performance comparison on large instances. . . . .	26
5	Chicago dataset characteristics. . . . .	28
6	Performance of BD-single-Pareto on Chicago dataset. . . . .	30

## Liste des figures

1	Network model of the MASFLP. . . . .	13
2	Chicago network and 797 nodes representing the census tracts (City of Chicago, 2018). . . . .	29
3	Facility locations and their coverage for Chicago network for level 0, $d = 1$ and $\lambda = 0\%$ with $m \in \{20, 40, 60, 100\}$ in figures (a), (b), (c), and (d), respectively. . . . .	33
4	Percentage of demand coverage with $m \in \{10, 20, 40, 60, 80, 100\}$ for different $d$ , $\lambda$ , and confinement level in figures (a), (b), and (c), respectively. . .	34
5	Type of coverage for varying $d$ , $\lambda$ , and confinement level in figures (a), (b), and (c), respectively. . . . .	35
6	Cost of immobility (CI) for all levels of confinement with $m = 20, 40, 60, 80$ facilities, in figures (a), (b), (c), (d), respectively. . . . .	36

# Avant-propos

Ce mémoire est écrit sous forme d'un article qui sera soumis à une revue scientifique. L'article a reçu l'autorisation de la direction du programme de M.Sc. ainsi que le consentement du co-auteur pour son utilisation.

# Remerciements

Je tiens tout d'abord à remercier mon directeur de recherche, Professeur Okan Arslan, pour l'opportunité de travailler sur ce projet, ses conseils judicieux qui ont aidé à guider mes efforts et aussi pour sa patience et sa disponibilité.

Je voudrais aussi remercier Taib et Taylor pour avoir lu et corrigé mon mémoire ainsi que leurs nombreux conseils pour améliorer mon style d'écriture.

Enfin, je voudrais exprimer ma reconnaissance à mes parents, mes frères, ainsi que mes amis pour leur encouragement et soutien constant tout au long de la maîtrise.





# Chapitre 1: Introduction

Les infrastructures publiques telles que les bureaux gouvernementaux, les centres médicaux, les stations de ravitaillement et les guichets automatiques offrent différents types de services aux citoyens. Par conséquent, leur emplacement a un impact sur leur disponibilité et surtout leur succès. Les citoyens peuvent visiter ces installations lors d'une visite isolée ou dans le cadre de leurs déplacements quotidiens, en suivant un itinéraire pré-planifié. Dans cet article, nous considérons les deux types de clients, dans le but de planifier l'emplacement des installations de service et de maximiser leur disponibilité, tout en respectant l'équité entre les citoyens.

L'optimisation de l'emplacement de ces installations vise à maximiser la demande couverte. Elle peut être stationnaire, comme dans les zones résidentielles et les lieux de travail, où les clients sont immobiles pendant de longues périodes, mais les clients peuvent aussi être mobiles et faire des visites pendant la période d'ouverture des installations. On commence par passer en revue les problèmes de la science de la localisation qui répondent aux deux types de demande. Hodgson (1990) introduit le problème de "*flow capturing location problem*" (FCLP), où la demande est considérée comme mobile et est définie en tant que paires origine-destination (OD). Ici, l'objectif est de couvrir la demande maximale en ouvrant un nombre donné d'installations. Berman et al. (1992) introduisent le problème de "*discretionary facility location problem*" (DSFLP), qui est structurellement le même que le FCLP. Les auteurs proposent une méthode de résolution basée sur un algorithme d'énumération implicite et présentent des résultats de calcul sur des réseaux aléatoires. Des applications réelles du FCLP sont étudiées par Hodgson et al. (1996) dans un réseau routier de la ville d'Edmonton. Dans la définition de base du FCLP, les conducteurs sont neutres quant à l'emplacement des installations et ne changent pas leurs trajets pré-planifiés pour visiter une installation. Le problème a connu un regain d'intérêt

dans la littérature et l’une de ses applications décrites est le problème de “*flow refueling location problem*” (FRLP) de Kuby et Lim (2005), dans lequel la couverture d’une demande nécessite d’intercepter un flux de véhicules plusieurs fois. Cela garantit la connectivité de la paire OD sans manquer de carburant. Les extensions et généralisations du FRLP prennent en compte les capacités des stations de ravitaillement (Upchurch et al., 2009) et la congestion routière (Riemann et al., 2015). Le FCLP peut être catégorisé en trois groupes en fonction du comportement du conducteur (Arslan et al., 2018): les conducteurs peuvent être neutres, coopératifs ou non coopératifs dans leur chemin pour visiter ou éviter les installations. Dans le cas de la coopération, Berman et al. (1995) considèrent que le conducteur s’écarte de ses déplacements pré-planifiés pour visiter les installations de service. Kim et Kuby (2012) mettent en œuvre la même idée pour le FRLP. Yıldız et al. (2016) développent un algorithme d’énumération implicite avec génération de colonnes pour le même problème. Lorsque les chauffeurs ne coopèrent pas, comme dans le cas des camionneurs en surpoids évitant de rencontrer des stations de pesage, le problème auquel nous sommes confrontés est alors un problème de capture de flux évasif (Marković et al., 2015). D’autres applications pertinentes incluent les emplacements des établissements de soins de santé. Taymaz et al. (2020) abordent le problème de la localisation des établissements de soins de santé pour les travailleurs mobiles, œuvrant dans les villes dans des conditions sévères qui affaiblissent leur santé. L’article propose un modèle stochastique pour localiser les cliniques sans rendez-vous et attribuer différents services en tenant compte de la demande mobile.

Alors que le FCLP capture le flux de la demande entre les paires OD, les “*covering location problems*” (CLP) sont utilisés pour localiser les installations en tenant compte de la couverture de la demande stationnaire. Selon les ressources disponibles, toute la demande peut être couverte en minimisant le nombre d’installations. Sinon, un maximum de demande peut être couvert en localisant un nombre donné d’installations. Les CLP sont largement utilisés

dans diverses applications, notamment la logistique humanitaire et la santé. Erkut et al. (2008) proposent un modèle pour localiser les emplacements des services médicaux d'urgence. Les auteurs améliorent trois modèles de couverture classiques en incluant une fonction de survie qui met en relation le temps de réponse et la probabilité de survie. Ils montrent que leur modèle produit des solutions plus réalistes que les modèles classiques d'emplacement de couverture maximale. Murali et al. (2012) introduisent un problème de localisation des installations avec capacité pour localiser les centres de distribution médicale en cas d'attaque biologique terroriste. Ils supposent que la satisfaction de la demande est liée à la distance et ils considèrent l'incertitude de la demande dans leur modèle. Les applications récentes du CLP incluent la localisation des installations de drones. Chauhan et al. (2019) introduisent le problème et proposent une approche heuristique en trois étapes pour le résoudre. Nous renvoyons à Snyder (2011) et García and Marín (2019) pour diverses applications du CLP ainsi que leurs extensions.

Le FCLP et le CLP font partie des nombreux modèles de localisation utilisés pour optimiser l'emplacement des installations. Turkoglu and Genevois (2020) fournissent une étude complète de la localisation des installations de service et les classent par application. Parmi les exemples cités, on trouve les services bancaires, les soins de santé, la restauration et le ravitaillement en carburant. Bien que ces modèles puissent être utilisés dans plusieurs contextes, leurs différents champs d'applications requièrent une couverture de la demande à leur origine et destinations, ainsi que la nécessité de capter les flux de demande sur les chemins OD. Par exemple, une routine quotidienne régulière d'un individu qui travaille commence à son domicile, puis continue avec un trajet aller-retour entre le travail et la maison. En fonction de ses heures de départ et d'arrivée, il peut trouver une installation de service à son origine, sur son trajet aller, ou à sa destination. Dans le même réseau, il y a aussi des demandes stationnaires qui sont localisées aux nœuds, et le processus de planification des installations de service doit prendre en compte les

deux types de demande. Une telle définition de la demande est applicable à l'emplacement de plusieurs types d'installations:

- *Les bureaux gouvernementaux:* tels que les services d'immigration, les services d'emploi et de retraite ou les services d'assurance maladie,
- *Les centres de test pendant une pandémie:* le but est de fournir à la population une possibilité de se faire tester à proximité de leur domicile, de leur école, de leur lieu de travail ou de leur trajet quotidien,
- *Les bureaux de vote.*

Même lorsque les clients sont à proximité des installations de service, leur accès y reste limité en raison de leur routine quotidienne et de leurs obligations professionnelles ou scolaires. Le but est donc de leur offrir la possibilité de bénéficier de ces services pendant leur temps disponible. À cette fin, nous introduisons le problème de “*maximum availability service facility location problem*” (MASFLP), qui localise les installations de service en maximisant leur disponibilité pour les clients. Une demande est définie comme une paire OD et elle peut être couverte à l'origine, à la destination ou sur le chemin aller-retour. La couverture est le temps nécessaire pour accéder à une installation et est délimitée par une borne supérieure. Cette définition de la demande nous permet de modéliser les clients qui se déplacent en véhicule privé ou en transports en commun ainsi que les clients stationnaires aux nœuds. La dimension temporelle est impliquée dans cette définition de la demande. Les clients peuvent avoir du temps libre à l'origine (par exemple, avant le travail ou l'école), sur leur trajet pour se rendre au travail, ou à leur destination (par exemple, pendant les pauses ou après le travail). Pour assurer l'équité, chaque point de demande ne peut être couvert que pendant un nombre d'heures limité. Cela garantit que les installations de service ne sont pas concentrées dans les régions densément peuplées et que toute la demande est traitée équitablement. Le MASFLP gère également la cannibalisation des flux (Hodgson, 1990) qui survient lorsque les installations sont situées à des intersections stratégiques,

avec des flux élevés, ce qui conduit à couvrir plusieurs fois les flux élevés et à ignorer les plus petits flux de demande. Des précisions supplémentaires sont présentées dans la section 2 de l'article.

Les méthodes de solution pour le FCLP et le CLP ont été largement explorées. Les algorithmes de décomposition de Benders (BD) (Benders, 1962) sont particulièrement adaptés à la structure de ces problèmes de localisation. Arslan et Karaşan (2016) utilisent la décomposition BD et proposent différentes implémentations de coupes pour résoudre le problème de l'emplacement des stations de charge pour véhicules électriques et hybrides rechargeables. Cordeau et al. (2019) introduisent une nouvelle approche basée sur la méthode BD pour résoudre des problèmes de couverture partielle de grande échelle et les problèmes de couverture maximale. De plus, leur algorithme est capable de résoudre des applications contenant des données massives. Les méthodes BD sont également utilisées dans d'autres applications. Zetina et al. (2019) présentent deux algorithmes exacts pour résoudre le problème de conception de réseau de multiproduit sans capacité à charge fixe. Ils montrent que leur algorithme fournit une accélération par rapport à CPLEX. Nous renvoyons à Costa (2005) et Rahmaniani et al. (2017) pour une revue de l'utilisation des algorithmes BD dans différents problèmes d'optimisation. D'autres méthodes de solution sont couvertes dans l'étude de Turkoglu and Genevois (2020).

#### *Contributions scientifiques du projet*

- Introduction d'un nouveau problème: "*maximum availability service location problem*", qui prend en compte à la fois la demande stationnaire et mobile dans une région urbaine, ainsi que l'équité géographique entre les individus.
- Présentation d'une formulation de programmation linéaire en nombres entiers mixtes pour le MASFLP.
- Développement d'un algorithme BD pour résoudre le modèle et de di-

verses techniques d'accélération, notamment les coupes multiples et les coupes Pareto-optimales. Résolution des sous-problèmes de façon analytique, et génération des coupes Pareto-optimales en tant qu'expressions de forme fermée.

- Conduite d'expériences informatiques approfondies pour évaluer l'efficacité et les performances des solutions proposées par rapport à CPLEX.
- Présentation de l'efficacité de l'algorithme proposé sur des réseaux aléatoires et d'une étude de cas dans la ville de Chicago, pour l'optimisation de l'emplacement des centres de test en situation de pandémie.

Les contributions sont détaillées dans le chapitre 2 du mémoire contenant l'article scientifique. Le travail sur cet article a été mené en collaboration avec mon directeur de recherche, Pr. Okan Arslan, qui m'a assisté pendant les étapes de conceptualisation et de méthodologie, ainsi que la revue et la correction du manuscrit.

Le reste du mémoire contient l'article dans le chapitre 2 et la conclusion et les directions pour des futurs travaux de recherche dans le chapitre 3.

# Chapitre 2: Article

## A Benders Decomposition Algorithm for the Maximum Availability Service Facility Location Problem

Ali Muffak<sup>a</sup>, Okan Arslan<sup>a</sup>

<sup>a</sup>HEC Montréal and CIRRELT, 3000 Chemin de la Côte-Sainte-Catherine, Montréal, QC H3T 2A7, Canada

---

### Abstract

This paper introduces the maximum availability service facility location problem, which integrates the set covering and flow capturing problems to capture both stationary and mobile demand in an urban region. The problem has applications in location of government offices, medical facilities and polling stations. We present a mixed-integer linear programming formulation and develop a Benders decomposition algorithm. We implement several acceleration techniques including multi-cut and Pareto-optimal cut generation. We construct these cuts analytically using closed-form expressions for subproblem solutions. Our best algorithm optimally solves instances with up to one thousand nodes, one million commuting customers and one hundred candidate facilities. We also conduct a case study with real data from the city of Chicago and show an application of our model for the location of medical facilities in a pandemic situation. We find that confinement restrictions in a pandemic do not significantly affect the total demand coverage, but facility layout may be significantly different under different confinement levels.

*Keywords:* location optimization, service facility, maximum availability, Benders decomposition, Pareto-optimal cut

---

### 1. Introduction

Service facilities such as government offices, medical centers, refueling stations and automatic teller machines offer various types of services to the public, and their location has an impact on their availability and ultimately their success. Individuals can visit such facilities on an independent trip or as part of their daily commute on their preplanned paths. In this paper, we consider both types of customers when planning for the location of service facilities and maximize their availability by respecting fairness among the individuals.

The location optimization of service facilities aims at maximizing the covered demand. The demand can be stationary, such as in residential areas or work places where the customers are



immobile for extended periods of time, or they can be mobile and travel during the period when facilities provide their service. We now review the problems in location science that address the two demand types. Hodgson (1990) introduces the flow capturing location problem (FCLP) where the demand is considered to be mobile and is defined as origin-destination (OD) pairs. The objective is to cover the maximum demand by opening a given number of facilities. Berman et al. (1992) independently introduce the discretionary service facility location problem, which is structurally the same as the FCLP. The authors propose a solution method based on branch-and-bound (B&B) algorithm and present computational results on random networks. Real-world applications of the FCLP are investigated by Hodgson et al. (1996) in a traffic network from the city of Edmonton. In the basic FCLP definition, the drivers are neutral to the location of facilities and do not change their preplanned paths to visit a facility. The problem has witnessed a surge of interest in the literature and one of the touted applications is the the flow refueling location problem (FRLP) by Kuby and Lim (2005), in which covering a demand requires intercepting a vehicle flow possibly for multiple times en route. This ensures the connectivity of the OD pair without running out of the fuel. Upchurch et al. (2009) extended the FRLP by including the capacities of refueling stations. The above FRLP models assume that the vehicles are half-fuelled at the beginning of their trip. Wen et al. (2014) introduced a general model that works with any level of starting fuel and with both one-way trips and round trips. The FRLP was also extended to include road congestion (Riemann et al., 2015). The FCLP can be categorized into three groups according to the drivers' behavior (Arslan et al., 2018): the drivers can be neutral, cooperative or non-cooperative to change their paths to visit or avoid the facilities. In the cooperative case, Berman et al. (1995) consider driver deviation from their preplanned trips to visit the service facilities and Kim and Kuby (2012) implement the same idea for the FRLP. Yıldız et al. (2016) develop a branch-and-price algorithm for the same problem. When the drivers are noncooperative, as in the case of overweight truck drivers avoiding to encounter weighing stations, the problem we face is then an evasive flow capturing problem (Marković et al., 2015). Other relevant applications include health care facility locations. Taymaz et al. (2020) address the problem of locating health care facilities for mobile workers, who work across cities under severe conditions that debilitate their health. The paper proposes a stochastic model to locate walk-in clinics and allocate different services by considering the mobile demand.

While the FCLP captures demand flow between OD pairs, covering location problems (CLP) are used to locate facilities by considering the coverage of stationary demand. Depending on the available resources, all the demand can be covered by minimizing the number facilities or a maximum amount of demand can be covered by locating a given number of facilities. Covering problems are extensively used in various applications including humanitarian logistics and health care. Erkut et al. (2008) propose a model for locating emergency medical service facilities. The authors enhance three classical covering models by including a survival function that puts in relation the response time and survival probability. They show that their model produces more realistic

solutions than the classic maximal covering location models. Murali et al. (2012) introduce a capacitated facility location problem to locate medical distribution centers in case of a bio-terror attack. They assume that demand satisfaction is related to distance and they consider demand uncertainty in their model. Recent applications of the CLP include facility location for drones. Chauhan et al. (2019) introduce the problem and propose a 3-stage heuristic approach to solve it. We refer to Snyder (2011) and García and Marín (2019) for various CLP applications and their extensions.

FCLP and CLP are among numerous location models used to optimize facility locations. Turkoglu and Genevois (2020) provide a comprehensive survey of service facility locations and categorize them by application, from banking and health care services to food and refueling applications. While these models can be used in multiple settings, various application contexts require the need to cover the demand at their origins and destinations as well as the need to capture the demand flow on the OD paths. In particular, a regular daily routine of a working individual starts at their home, continues with a commute and finally a journey from work back to home. Depending on their departure and arrival times, they may find a service facility at their origin, on their commute route or at their destination. In the same network, there are also stationary demands that are located at nodes and the service facility planning process needs to take into consideration both types of demand. Such a demand definition is applicable in the location of several facility types:

- *Government offices:* such as immigration services, employment and pension services or health insurance services,
- *Testing facility clinics during a pandemic:* The goal is to provide the population with an opportunity to get tested in close proximity to their homes, schools, workplaces, or on their daily commute,
- *Polling stations for voting.*

Even when the customers are in close proximity to the service facilities, they have limited access to these facilities due to their daily routine and work or school commitments. The aim is to provide customers the opportunity to benefit from these services during their available time. To this end, we introduce *the maximum availability service facility location problem* (MASFLP), which locates service facilities by maximizing their availability to the customers. A demand is defined as an OD pair and it can be covered at the origin, at the destination, or on their way from their origin to the destination. The coverage is defined in terms of the time they have access to at least one facility and is bounded above by a limit. This demand definition allows us to model the customers who commute using their private vehicles or public transportation as well as the stationary customers at nodes. Time dimension is involved in this demand definition. Customers can have available

time at their origin (for example, before work or school), on their journey to work, or at their destination (for example, during breaks or after work). To ensure fairness, each demand point can only be covered for a limited number of hours. This guarantees that the service facilities are not concentrated in densely populated regions and all the demand are treated fairly. The MASFLP also handles flow cannibalization (Hodgson, 1990) that arises when facilities are located at strategic intersections with high flow, which leads to covering high flows multiple times and ignoring smaller demand flows. Further elaborations are presented in Section 2.

Solution methods for the FCLP and the CLP have been explored extensively, and Benders decomposition (BD) algorithms (Benders, 1962) are especially suited for the structure of these location problems. Arslan and Karaşan (2016) use BD decomposition and proposed different cut implementations to solve the charging station location problem with electric vehicles and plug-in hybrid vehicles. Cordeau et al. (2019) introduce a new approach based on BD to solve large scale partial set covering problems and maximal covering problems. Their algorithm is capable of solving massive data instances. BD methods are also used in other applications. Zetina et al. (2019) present two exact algorithms to solve the multicommodity uncapacitated fixed-charge network design problem. They show that their algorithm provides an acceleration when compared to CPLEX. We refer to Costa (2005) and Rahmaniani et al. (2017) for a review on the application of BD algorithms in different optimization problems. Other solution methods are covered in the survey by Turkoglu and Genevois (2020).

The location optimization of service facility requires consideration of various factors. The main contributions of this paper are as follows:

- We introduce the maximum availability service facility location problem (MASFLP) by considering both stationary and mobile demand in an urban region. We also consider geographical fairness among the individuals.
- We present a mixed-integer linear programming formulation for the MASFLP.
- We develop a BD algorithm to solve the model and test various acceleration techniques including multi-cut and Pareto-optimal cut generation. We exploit the subproblem structure to solve them analytically and generate Pareto-optimal cuts as closed-form expressions.
- We conduct extensive computational experiments to evaluate the effectiveness and performance of our proposed solutions compared to CPLEX.
- We demonstrate the efficiency of our algorithm on random networks and present a case study in the city of Chicago for testing center location optimization in a pandemic situation.

The rest of the paper is organized as follows. In Section 2, we introduce the notation and the mathematical model. We present the BD algorithm and the analytical solutions of the subproblem

in Section 3, the computational experiments in Section 4, and we conduct a case study in Section 5. Finally, we conclude and offer directions for future work in Section 6.

## 2. Mathematical model

We now introduce the problem and present a mathematical formulation for the MASFLP.

### 2.1. Problem definition and notation

Let  $K$  be the set of candidate facilities and  $m$  be the number of facilities to locate. Let  $Q$  be the set of customer demands, and  $G = (N, A)$  be the transportation network where  $N$  is the set of nodes and  $A = \{(i, j) : i, j \in N, i \neq j\}$  is the set of directed arcs. The length of arc  $(i, j) \in A$  is  $l_{ij}$ . We assume that the distance matrix satisfies the triangular inequality. Each customer demand  $q \in Q$  is defined by  $\langle o_q, d_q, f_q, t_q^o, t_q^d, t_q^p, \lambda_q \rangle$ , where  $o_q$  and  $d_q$  are the origin and destination nodes, respectively, and  $f_q$  is the volume of customers living at  $o_q$ , working at  $d_q$  and commuting in between. Parameters  $t_q^o, t_q^d$  and  $t_q^p$  represent the customers' available time during the business hours at the origin, at the destination, and on the OD path, respectively, and  $\lambda_q$  is the customers' deviation tolerance from their preplanned OD path. A non-commuting demand residing at  $o_q$  can be represented by setting  $d_q = o_q$ . Each candidate facility  $k \in K$  has a coverage range of  $r_k$ . A facility  $k$  covers demand at node  $i$  if  $l_{ik} \leq r_k$ , and on path between  $o_q$  and  $d_q$  if  $l_{o_q k} + l_{k d_q} \leq (1 + \lambda)l_{o_q d_q}$ . For a  $q \in Q$ , the maximum contribution to the objective function can be at most  $t_{max}$ , which ensures that the service is provided fairly to all demand in the network. The service is defined as time availability and not as binary, hence the higher the availability the higher the service provided. Times  $t_q^o, t_q^d$  and  $t_q^p$  can be regarded as a weight for each demand  $q \in Q$  and do not encourage flow cannibalization, which is handled by binary location variables defined in section 2.2 as introduced by (Hodgson, 1990). Let  $N_p$  the set of potential locations on path  $p$ ,  $N_o$  the set of potential locations covering origin  $o$ , and  $N_d$  the set of potential locations covering destination  $d$ .

**Definition 1.** *The MASFLP is defined as selecting a subset of  $K$  to open such that the total availability provided to the demand is maximized and the maximum contribution of each demand is at most  $t_{max}$ .*

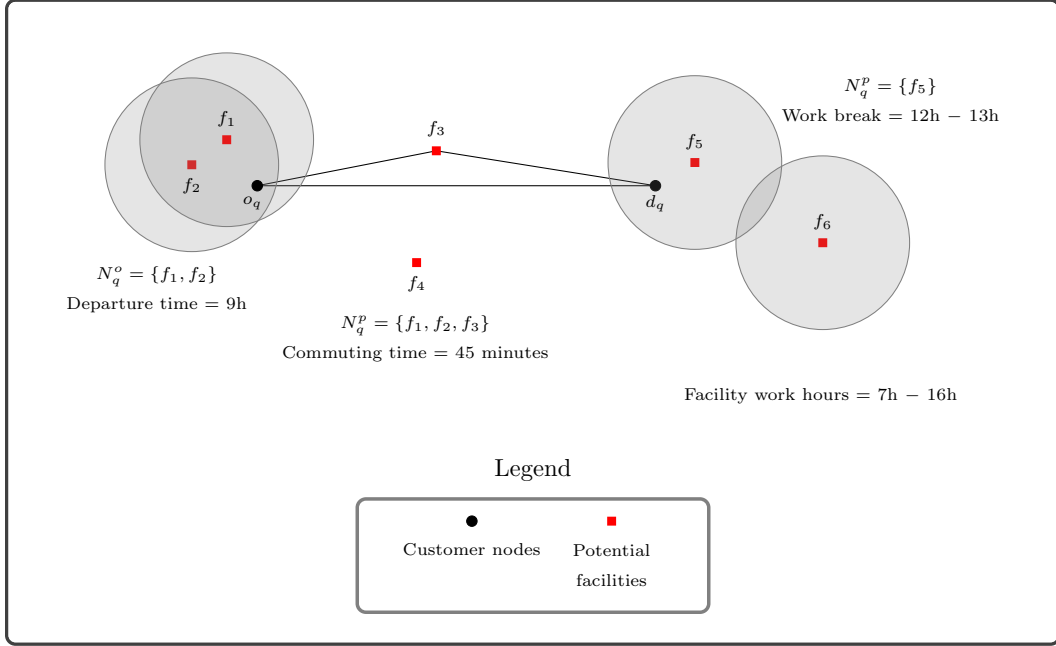


Figure 1: Network model of the MASFLP.

Figure 1 shows an example of a demand on a small network. Observe that demand  $q$  can be covered at origin  $o_q$  by facilities  $f_1$  and  $f_2$  for  $t_q^o = 2$  hours. Availability time  $t_q^o$  is the difference between the facility opening hour and the departure time. Demand  $q$  can also be covered on the OD path by facilities  $f_1$ ,  $f_2$  and  $f_3$  for a fixed amount of time, which is taken as  $t_q^p = 45$  minutes and around the destination  $d_q$  by facility  $f_5$  for  $t_q^d = 1$  hour during the work break. Demand  $q$  cannot be covered by  $f_4$  because the driver is intolerant to high deviations and cannot be covered by  $f_6$  either because node  $d_q$  is not within the facility's range.

**Remark 1.** If  $o_q = d_q$ ,  $t_q^p = t_q^d = 0$  for all  $q \in Q$ , and  $t_{max} = \max_{q \in Q} f_q$ , the MASFLP reduces to the MCLP.

**Remark 2.** If  $t_q^o = t_q^d = 0$  and  $t_q^p = 1$  for all  $q \in Q$  and  $t_{max} = \max_{q \in Q} f_q$ , the MASFLP reduces to the FCLP.

Therefore, the MASFLP generalizes the MCLP and the FCLP and is NP-hard.

## 2.2. Mathematical model

We use the following decision variables to formulate the MASFLP.

$x_k = 1$  if a facility is located at location  $k$ , 0 otherwise,

$y_q^o = 1$  if demand  $q$  is captured at origin  $o_q$ , 0 otherwise,

$y_q^d = 1$  if demand  $q$  is captured at destination  $d_q$ , 0 otherwise,

$y_q^p = 1$  if demand  $q$  is captured on path  $p_q$ , 0 otherwise and

$\theta_q$  is the time that a service facility is available for demand  $q$ .

The MASFLP is then formulated as the following MILP.

$$\text{maximize } \sum_{q \in Q} \theta_q f_q \quad (1)$$

$$\text{subject to } \sum_{k \in K} x_k = m \quad (2)$$

$$\theta_q \leq t_{max} \quad q \in Q \quad (3)$$

$$\theta_q \leq t_q^o y_q^o + t_q^d y_q^d + t_q^p y_q^p \quad q \in Q \quad (4)$$

$$\sum_{k \in N_q^o} x_k \geq y_q^o \quad q \in Q \quad (5)$$

$$\sum_{k \in N_q^d} x_k \geq y_q^d \quad q \in Q \quad (6)$$

$$\sum_{k \in N_q^p} x_k \geq y_q^p \quad q \in Q \quad (7)$$

$$\theta_q \geq 0 \quad q \in Q \quad (8)$$

$$x_k \in \{0, 1\} \quad k \in K \quad (9)$$

$$y_q^o, y_q^d, y_q^p \in \{0, 1\} \quad q \in Q. \quad (10)$$

The objective function maximizes total availability of facilities to the customers. Constraints (3) ensure that the available time of demand  $q \in Q$  to the service does not exceed a maximum amount of time  $t_{max}$ . Constraints (4) ensure that the available time is correctly calculated. Constraints (5), (6), and (7) ensure that a demand is covered only if a facility is open within the coverage range of its origin and destination or on an OD path. Finally, constraints (8), (9), and (10) define the domain of variables. It is straightforward to show that, without loss of generality, we can relax the integrality requirement of the  $y_q^o$ ,  $y_q^d$ , and  $y_q^p$  variables. We refer to the formulation with relaxed  $y$  variables as P.

## 3. Benders Decomposition

In this section, we develop a BD algorithm (Benders, 1962) for solving the P model. BD is a decomposition algorithm, in which the continuous variables are projected out from the formulation

and an exponential number of constraints are appended instead. These constraints correspond to the extreme points and rays of the linear programming model, which is obtained by fixing the integer variables in the original formulation. Adding all such cuts is impractical, therefore they are added to the formulation as needed. For more information on various implementation details of the algorithm, we refer the reader to Rahmaniani et al. (2017). We now present the reformulation of our problem and introduce analytical solutions of the subproblems and different cut generation strategies to accelerate the algorithm.

### 3.1. Benders subproblem

By fixing the variable  $x$  in the P formulation to  $\hat{x} \in \{0, 1\}^{|K|}$ , we obtain a linear programming (LP) model, which we refer to as subproblem  $SP(\hat{x})$ .

$$\text{maximize} \quad \sum_{q \in Q} \theta_q f_q \quad (11)$$

$$\text{subject to} \quad \theta_q \leq t_{max} \quad q \in Q \quad (12)$$

$$\theta_q - t_q^o y_q^o - t_q^d y_q^d - t_q^p y_q^p \leq 0 \quad q \in Q \quad (13)$$

$$y_q^o \leq \sum_{k \in N_q^o} \hat{x}_k \quad q \in Q \quad (14)$$

$$y_q^d \leq \sum_{k \in N_q^d} \hat{x}_k \quad q \in Q \quad (15)$$

$$y_q^p \leq \sum_{k \in N_q^p} \hat{x}_k \quad q \in Q \quad (16)$$

$$y_q^o \leq 1 \quad q \in Q \quad (17)$$

$$y_q^d \leq 1 \quad q \in Q \quad (18)$$

$$y_q^p \leq 1 \quad q \in Q \quad (19)$$

$$\theta_q, y_q^o, y_q^d, y_q^p \geq 0 \quad q \in Q. \quad (20)$$

Note that the subproblem is closed and bounded and therefore feasibility cuts are not needed and optimality cuts are enough to ensure convergence of the algorithm. Let  $\alpha, \beta, \gamma, \mu, \rho, \phi, \sigma, \delta$  be the dual variables associated with constraints (12)–(19), respectively. Then the dual subproblem referred to as  $DSP(\hat{x})$  is the following:

$$\text{minimize} \quad \sum_{q \in Q} t_{max} \alpha_q + \sum_{\substack{q \in Q \\ k \in N_q^o}} \hat{x}_k \gamma_q + \sum_{\substack{q \in Q \\ k \in N_q^d}} \hat{x}_k \mu_q + \sum_{\substack{q \in Q \\ k \in N_q^p}} \hat{x}_k \rho_q + \sum_{q \in Q} \phi_q + \sum_{q \in Q} \sigma_q + \sum_{q \in Q} \delta_q \quad (21)$$

$$\text{subject to} \quad \alpha_q + \beta_q \geq f_q \quad q \in Q \quad (22)$$

$$\gamma_q - t_q^o \beta_q + \phi_q \geq 0 \quad q \in Q \quad (23)$$

$$\mu_q - t_q^d \beta_q + \sigma_q \geq 0 \quad q \in Q \quad (24)$$

$$\rho_q - t_q^p \beta_q + \delta_q \geq 0 \quad q \in Q \quad (25)$$

$$\alpha_q, \beta_q, \gamma_q, \mu_q, \rho_q, \phi_q, \sigma_q, \delta_q \geq 0 \quad q \in Q. \quad (26)$$

### 3.2. Benders master problem

Let  $\mathcal{D}(\text{DSP})$  denote the set of extreme points of  $\text{DSP}(\hat{x})$ . We construct the master problem referred to as MP as follows:

$$\text{maximize } \eta \quad (27)$$

$$\begin{aligned} \text{subject to } \eta \leq & \sum_{q \in Q} t_{max} \alpha_q + \sum_{\substack{q \in Q \\ k \in N_q^o}} x_k \gamma_q + \sum_{\substack{q \in Q \\ k \in N_q^d}} x_k \mu_q \\ & + \sum_{\substack{q \in Q \\ k \in N_q^p}} x_k \rho_q + \sum_{q \in Q} \phi_q + \sum_{q \in Q} \sigma_q + \sum_{q \in Q} \delta_q \quad (\alpha, \gamma, \mu, \rho, \phi, \sigma, \delta) \in \mathcal{D}(\text{DSP}) \end{aligned} \quad (28)$$

$$\sum_{k \in K} x_k = m \quad (29)$$

$$x_k \in \{0, 1\} \quad k \in K. \quad (30)$$

To handle the exponential number of constraints in the MP (constraints (28)), we use a branch-and-cut approach. Cuts are added to the MP in the form of inequality (28) by solving the  $\text{DSP}(\hat{x})$ . The MP is solved in a single B&B tree similar to Codato and Fischetti (2006).

### 3.3. Subproblem solution

Given  $\hat{x}$ ,  $\text{DSP}(\hat{x})$  is an LP and can be solved using a solver. In this section, we present analytical solutions of  $\text{DSP}(\hat{x})$  without the need to build and solve an LP. First, note that the dual subproblem  $\text{DSP}(\hat{x})$  can be decomposed based on the demand  $q \in Q$ . We refer to the following decomposed dual subproblem formulation as  $\text{DSP}_q(\hat{x})$ .

$$\text{minimize } t_{max} \alpha_q + \sum_{k \in N_q^o} \hat{x}_k \gamma_q + \sum_{k \in N_q^d} \hat{x}_k \mu_q + \sum_{k \in N_q^p} \hat{x}_k \rho_q + \phi_q + \sigma_q + \delta_q \quad (31)$$

$$\text{subject to } \alpha_q + \beta_q \geq f_q \quad (32)$$

$$\gamma_q - t_q^o \beta_q + \phi_q \geq 0 \quad (33)$$

$$\mu_q - t_q^d \beta_q + \sigma_q \geq 0 \quad (34)$$

$$\rho_q - t_q^p \beta_q + \delta_q \geq 0 \quad (35)$$

$$\alpha_q, \beta_q, \gamma_q, \mu_q, \rho_q, \phi_q, \sigma_q, \delta_q \geq 0. \quad (36)$$



We now start constructing a closed-form solution for  $\text{DSP}_q(\hat{x})$ . For conciseness, let  $\hat{x}_q^o = \sum_{k \in N_q^o} \hat{x}_k$ ,  $\hat{x}_q^d = \sum_{k \in N_q^d} \hat{x}_k$ , and  $\hat{x}_q^p = \sum_{k \in N_q^p} \hat{x}_k$ .

**Proposition 1.** *Constraint (32) is always active in an optimal solution of  $\text{DSP}_q(\hat{x})$ .*

PROOF. Observe that  $\text{SP}(\hat{x})$  can be decomposed based on  $q$ . For a given  $\hat{q} \in Q$ , consider the primal-dual subproblem pair. Constraint (32) in the  $\text{DSP}_q(\hat{x})$  corresponds to the non-negative  $\theta_q$  variable in the MP. When  $\theta_q = 0$ , the particular demand cannot be covered and therefore the objective function value is zero. The dual objective function value therefore equals zero due to strong duality. Observe that the solution  $\alpha_q = \phi_q = \sigma_q = \delta_q = 0$ ,  $\beta_q = f_q$ ,  $\gamma_q = t_0\beta_q$ ,  $\mu_q = t_d\beta_q$  and  $\rho_q = t_p\beta_q$  is feasible and has an objective function value of zero. Therefore it is optimal and satisfies constraint (32) at equality. Now, consider the case with  $\theta_q > 0$ . Constraint (32) is then always active due to complementary slackness conditions.  $\square$

Proposition 1 implies that  $\alpha_q = f_q - \beta_q$  and variable  $\alpha_q$  can be projected out from the formulation by replacing this term in the objective function. We then obtain the following equivalent model.

$$\text{maximize } t_{max}\beta_q - \hat{x}_q^o\gamma_q - \hat{x}_q^d\mu_q - \hat{x}_q^p\rho_q - \phi_q - \sigma_q - \delta_q \quad (37)$$

$$\text{subject to } \gamma_q + \phi_q \geq t_q^o\beta_q \quad (38)$$

$$\mu_q + \sigma_q \geq t_q^d\beta_q \quad (39)$$

$$\rho_q + \delta_q \geq t_q^p\beta_q \quad (40)$$

$$f_q \geq \beta_q \quad (41)$$

$$\beta_q, \gamma_q, \mu_q, \rho_q, \phi_q, \sigma_q, \delta_q \geq 0. \quad (42)$$

Note that the nonnegativity of  $\alpha_q$  induces constraint (41). The objective function is also modified to a maximization to better see the multidimensional knapsack nature of the model.

For fixed  $\hat{x}$  and a given  $q \in Q$ , we define  $g_q(\hat{x}) = t_{max} - t_o \min\{\hat{x}_q^o, 1\} - t_d \min\{\hat{x}_q^d, 1\} - t_p \min\{\hat{x}_q^p, 1\}$ , which represents the gap between  $t_{max}$  and the potential availability of facilities for demand  $q$ . If  $g_q(\hat{x}) < 0$ , the existing network of facilities can provide more availability than  $t_{max}$  and If  $g_q(\hat{x}) > 0$ , the availability of the facilities is less than  $t_{max}$  for  $q$ . We are now ready to present a closed-form solution for the  $\text{DSP}_q(\hat{x})$ .

**Proposition 2.** Given  $\hat{x} \in \{0, 1\}^{|K|}$  and a demand  $q \in Q$ , the following is an optimal solution of the  $DSP_q(\hat{x})$ :

$$\beta_q = \begin{cases} f_q & \text{if } g_q(\hat{x}) \geq 0 \\ 0 & \text{otherwise} \end{cases}$$

$$\gamma_q = \begin{cases} t_q^o f_q & \text{if } g_q(\hat{x}) \geq 0 \text{ and } \hat{x}_q^o \leq 1 \\ 0 & \text{otherwise} \end{cases}$$

$$\mu_q = \begin{cases} t_q^d f_q & \text{if } g_q(\hat{x}) \geq 0 \text{ and } \hat{x}_q^d \leq 1 \\ 0 & \text{otherwise} \end{cases}$$

$$\rho_q = \begin{cases} t_q^p f_q & \text{if } g_q(\hat{x}) \geq 0 \text{ and } \hat{x}_q^p \leq 1 \\ 0 & \text{otherwise} \end{cases}$$

$$\phi_q = t_q^o f_q - \gamma_q$$

$$\sigma_q = t_q^d f_q - \mu_q$$

$$\delta_q = t_q^p f_q - \rho_q$$

□

PROOF. The constructed solution is feasible. Observe that the objective function coefficients of  $\gamma$  and  $\phi$  variables in model (37)–(42) are negative and they only appear in constraint (38), which implies that there exists an optimal solution satisfying constraint (38) at equality, that is  $\gamma_q + \phi_q = t_o \beta_q$ . Therefore, the objective function contribution of  $\gamma$  and  $\phi$  is  $-\hat{x}_q^o \gamma_q - \phi_q = -\min\{\hat{x}_q^o, 1\} t_o \beta_q$ . With a similar reasoning for the other variables, the objective function can be restated as  $t_{max} \beta_q - \min\{\hat{x}_q^o, 1\} t_o \beta_q - \min\{\hat{x}_q^d, 1\} t_d \beta_q - \min\{\hat{x}_q^p, 1\} t_p \beta_q$ . Hence, the optimal objective function value is zero if  $g_q(\hat{x}) := t_{max} - \min\{\hat{x}_q^o, 1\} t_o - \min\{\hat{x}_q^d, 1\} t_d - \min\{\hat{x}_q^p, 1\} t_p \leq 0$ . If  $g_q(\hat{x}) > 0$ , we have  $\beta_q = f_q$ . Due to the knapsack nature between the remaining variables, the conditions follow. □

In the following, we present three Benders cut selection schemes: single-cut, multi-cut and Pareto-optimal cut.

### 3.4. Benders cut selection scheme 1: single-cut

For a given  $\hat{x}$ , the dual values are computed according to proposition 2, then a cut is added to the MP at each iteration in the form of inequality (28).

### 3.5. Benders cut selection scheme 2: multi-cut

To implement the multi-cut scheme, we need to modify the master problem. A new set of variables  $\eta_q$  is introduced to the MP, each of which approximates the cost of a decomposed subproblem. The Multiple-cut generation scheme is implemented and is proved to be efficient in various studies including de Camargo et al. (2008) and You and Grossmann (2013). Let  $\eta_q$  be the variable associated with  $DSP_q(\hat{x})$ , and  $\mathcal{D}(DSP_q)$  the set of extreme points of the dual problems  $DSP_q$ . The modified master problem is formulated as follows,

$$\text{maximize } \sum_{q \in Q} \eta_q \quad (43)$$

$$\begin{aligned} \text{subject to } \eta_q \leq & t_{max} \alpha_q + \sum_{k \in N_q^o} x_k \gamma_q + \sum_{k \in N_q^d} x_k \mu_q \\ & + \sum_{k \in N_q^p} x_k \rho_q + \phi_q + \sigma_q + \delta_q \quad (\alpha, \gamma, \mu, \rho, \phi, \sigma, \delta) \in \mathcal{D}(DSP_q), q \in Q \end{aligned} \quad (44)$$

$$\sum_{k \in K} x_k = m \quad (45)$$

$$x_k \in \{0, 1\} \quad k \in K. \quad (46)$$

For a given  $\hat{x}$ , the values of the dual variables for each subproblem are computed according to Proposition 2 and each subproblem solution represents an extreme point used to generate a cut.

### 3.6. Benders cut selection scheme 3: Pareto-optimal cut

Generating effective cuts that can reduce the number of iterations is highly important. As we observe in Proposition 2, the subproblem can have multiple optimal values. In fact, when  $\hat{x}_q^o = 1$ ,  $\gamma_q$  and  $\phi_q$  values are interchangeable, which implies that infinitely many different cuts can be generated from the same  $\hat{x}$  solution. With the objective of generating stronger cuts by selecting one among these alternative cuts, we now investigate the Pareto-optimal cut generation scheme (Magnanti and Wong, 1981). Let  $\mathcal{X}$  be the feasible solution set of the master problem,  $opt(DSP(\hat{x}))$  be the optimal objective function value of problem  $DSP(\hat{x})$ , and the function  $\mathcal{C}(x, d)$  be defined as follows:

$$\mathcal{C}(x, d) = \sum_{q \in Q} t_{max} \alpha_q + \sum_{\substack{q \in Q \\ k \in N_q^o}} x_k \gamma_q + \sum_{\substack{q \in Q \\ k \in N_q^d}} x_k \mu_q + \sum_{\substack{q \in Q \\ k \in N_q^p}} x_k \rho_q + \sum_{q \in Q} \phi_q + \sum_{q \in Q} \sigma_q + \sum_{q \in Q} \delta_q,$$

where we use  $d = (\alpha, \gamma, \mu, \rho, \phi, \sigma, \delta)$  to refer to dual variables of  $DSP(x)$ , for conciseness.

In the Pareto-optimal cut scheme, we only add non-dominated cuts. A cut generated by the dual solution  $\bar{d}$  is considered to be dominated by the cut generated by the dual solution  $\tilde{d}$ , if and only if  $\mathcal{C}(x, \bar{d}) \leq \mathcal{C}(x, \tilde{d})$  for all  $x \in \mathcal{X}$  with a strict inequality for at least one of the points (Magnanti and Wong, 1981). Solving the following LP allows us to obtain Pareto-optimal cuts.

$$\text{minimize } \mathcal{C}(\bar{x}, d) \quad (47)$$

$$\text{subject to } (22) - (26)$$

$$\mathcal{C}(\hat{x}, d) = \text{opt}(DSP(\hat{x})). \quad (48)$$

We refer to the formulation above as  $MW(\hat{x}, \bar{x})$ , where  $\bar{x}$ , referred to as the core point, is an interior point of the convex hull of  $\mathcal{X}$ . The initial core point is a vector of length  $|K|$  and values  $\frac{m}{|K|}$  for each dimension. Similar to Papadakos (2008), the core point is updated after each iteration and takes the value of the average of the previous iteration and the current MP solution.

### 3.7. Magnanti-Wong problem solution

The  $MW(\hat{x}, \bar{x})$  can be decomposed based on demand  $q \in Q$ . Let  $\bar{x}_q^o = \sum_{k \in N_q^o} \bar{x}_k$ ,  $\bar{x}_q^d = \sum_{k \in N_q^d} \bar{x}_k$ , and  $\bar{x}_q^p = \sum_{k \in N_q^p} \bar{x}_k$ . We refer to the problem below as  $MW_q(\hat{x}, \bar{x})$ .

$$\text{minimize } t_{max} \alpha_q + \bar{x}_q^o \gamma_q + \bar{x}_q^d \mu_q + \bar{x}_q^p \rho_q + \phi_q + \sigma_q + \delta_q \quad (49)$$

$$\text{subject to } \alpha_q + \beta_q \geq f_q \quad (50)$$

$$\gamma_q - t_q^o \beta_q + \phi_q \geq 0 \quad (51)$$

$$\mu_q - t_q^d \beta_q + \sigma_q \geq 0 \quad (52)$$

$$\rho_q - t_q^p \beta_q + \delta_q \geq 0 \quad (53)$$

$$\mathcal{C}(\hat{x}, d) = \text{opt}(DSP(\hat{x})) \quad (54)$$

$$d_q \geq 0. \quad (55)$$

The analytical solution of the  $MW_q(\hat{x}, \bar{x})$  is as follows:

**Proposition 3.** *Given  $\hat{x} \in \{0, 1\}^{|K|}$  and a demand  $q \in Q$ , the following is an optimal solution of the  $DSP_q(\hat{x})$ :*

$$\alpha_q = \begin{cases} 0 & \text{if } g_q(\hat{x}) \geq 0 \\ f_q & \text{otherwise} \end{cases}$$

$$\begin{aligned}
\beta_q &= \begin{cases} f_q & \text{if } g_q(\hat{x}) \geq 0 \\ 0 & \text{otherwise} \end{cases} \\
\gamma_q &= \begin{cases} t_q^o f_q & \text{if } (g_q(\hat{x}) \geq 0 \text{ and } \hat{x}_q^o = 0) \text{ or } (g_q(\hat{x}) \geq 0 \text{ and } \hat{x}_q^o = 1 \text{ and } \bar{x}_q^o \leq 1) \\ 0 & \text{otherwise} \end{cases} \\
\mu_q &= \begin{cases} t_q^d f_q & \text{if } (g_q(\hat{x}) \geq 0 \text{ and } \hat{x}_q^d = 0) \text{ or } (g_q(\hat{x}) \geq 0 \text{ and } \hat{x}_q^d = 1 \text{ and } \bar{x}_q^d \leq 1) \\ 0 & \text{otherwise} \end{cases} \\
\rho_q &= \begin{cases} t_q^p f_q & \text{if } (g_q(\hat{x}) \geq 0 \text{ and } \hat{x}_q^p = 0) \text{ or } (g_q(\hat{x}) \geq 0 \text{ and } \hat{x}_q^p = 1 \text{ and } \bar{x}_q^p \leq 1) \\ 0 & \text{otherwise} \end{cases} \\
\phi_q &= t_q^o f_q - \gamma_q \\
\sigma_q &= t_q^d f_q - \mu_q \\
\delta_q &= t_q^p f_q - \rho_q
\end{aligned}$$

□

The correctness of Proposition 3 follows from Proposition 2 and similar multi-dimensional knapsack arguments. For sake of conciseness and to avoid repetition, we omit the details here.

#### 4. Computational Study

We now present the data, the design of experiments, and the performance of our algorithms. We present four different cut selection schemes and compare the solution efficiency of the BD algorithm to that of P model solved using CPLEX without any decomposition. We also carry out a case study using our best performing algorithm on a real-world Chicago dataset and discuss managerial findings. All the experiments are performed on a desktop computer with a 2.80 GHz 10-core Intel Core i9-10900F processor and 64GB of RAM, running 64-bit Windows operating system. The algorithms were implemented using Python 3.7.7 and the Python API of CPLEX 12.10.0.

##### 4.1. Design of Experiments

We have randomly generated nine different networks with a number of nodes  $n$  going from 100 to 1000 by increments of 100. The node coordinates are randomly selected in the interval  $[0, 25]$ . The demands are generated between all pairs of nodes and the customer volume  $f$  is assigned randomly in  $[1, 100]$  and rounded to the nearest integer. We have coverage distance  $d \in \{1, 3, 5\}$

and driver tolerance  $\lambda \in \{10\%, 30\%, 50\%\}$ . Sets  $N_o$ ,  $N_d$  and  $N_p$  are constructed accordingly. A work day is divided into 30 minute intervals for a total duration of 8 hours and we generate  $t_q^o, t_q^d$ , and  $t_q^p$  randomly in  $[1, 6]$ ,  $[1, 2]$ , and  $[1, 4]$ , respectively, and rounding to the nearest integer. We set  $t_{max}$  to 8, and ensure that for any demand  $q$ ,  $t_o + t_p + t_d \leq 8$ . All nodes are considered as potential facility locations and the number of OD pairs in each network is  $n^2$ . We set the maximum number of open facilities  $m \in \{5, 10, 15, 20, 30, 40, 50, 75, 100\}$ . Using nine randomly generated networks and these settings, we test the performance of the BD algorithm and compare different cut implementation schemes. All performance results presented in the tables hereafter represent the average performance on  $d$  and  $\lambda$ .

#### 4.2. Computational Results

In this section, we first present the performance of constructing the subproblem solutions analytically as opposed to building an LP model and solving in CPLEX. We then compare different BD implementations using closed-form solutions presented in Section 3 with the implementation on CPLEX without any decomposition. We consider five implementations:

- CPLEX: the MILP is solved using CPLEX directly without any decomposition.
- BD-single: single-cut implementation where the subproblem is solved analytically.
- BD-multi: multi-cut implementation where the subproblem is solved analytically.
- BD-single-Pareto: single-cut implementation where the subproblem is solved analytically and only Pareto-optimal cuts are added.
- BD-multi-Pareto: multi-cut implementation where the subproblem is solved analytically and only Pareto-optimal cuts are added.

In Table 1, we present the results of the performance of BD-single with subproblems solved using LPs and BD-single with subproblems solved analytically. We consider four network sizes from 100 to 400 and the number of facility locations considered is 5, 10, or 15. The three leftmost columns represent the instance setting and solution;  $n$  is the number of nodes in the network,  $m$  is the number of facility locations, and “Opt. Sol.” is the optimal objective function value of the corresponding instance. Columns 4 – 7 are the total solution time, the subproblem solution time, the number of subproblems, and lastly the average subproblem solution time, respectively, all in seconds (s). The average solution time for the BD-single with subproblems solved using LPs and BD-single with subproblems solved analytically is 251.9 and 33.8 seconds, respectively. BD-single with subproblems solved analytically is significantly more efficient and the acceleration increases more for larger networks.

We now present the results of the four BD implementations using analytical solutions and use CPLEX as a benchmark to compare the performance of these algorithms. The computational

Table 1: Comparison of BD subproblem solved analytically and subproblem solved using LPs.

Instance			BD-single (subproblems solved using LPs)				BD-single (subproblems solved analytically)			
$n$	$m$	Opt. Sol. ( $10^6$ )	Total Sol. Time (s)	Subp. Sol. Time (s)	# Subproblems	Avg. Subp. Sol. Time (s)	Total Sol. Time (s)	Subp. Sol. Time (s)	# Subproblems	Avg. Subp. Sol. Time (s)
100	5	3.17	5.0	4.9	5	1.0	1.3	1.2	6	0.2
	10	3.29	13.0	12.9	12	1.0	5.5	5.4	23	0.2
	15	3.39	35.2	35.2	28	1.3	30.2	29.9	121	0.3
200	5	12.35	55.1	55.0	4	13.8	6.7	6.7	4	1.7
	10	12.60	73.7	73.7	6	12.3	22.8	22.7	14	1.6
	15	12.82	238.0	237.9	17	14.0	60.3	60.1	33	1.8
300	5	27.69	166.0	165.9	3	55.3	15.8	15.7	3	5.2
	10	28.13	329.8	329.7	5	66.0	29.3	29.2	5	5.9
	15	28.53	331.1	331.1	5	66.2	31.4	31.3	6	5.2
400	5	49.12	509.9	509.9	3	170.0	37.5	37.4	3	12.5
	10	49.70	759.8	759.8	4	190.0	53.8	53.8	4	13.4
	15	50.18	1010.7	1010.7	5	202.1	111.4	111.3	9	12.4

performances are shown in Table 2. The column “Instance” presents the network size, the number of facility locations and the objective function value. The next column “CPLEX” shows the solution time and the gap (%) using CPLEX implementation. The gap is defined as  $(UB - LB)/UB * 100$ , where UB and LB are upper and lower bounds, respectively. For each of the BD implementations, we present the number of iterations under the column “# Iterations”, the total number of cuts under “# Cuts”, the total subproblem solution time and the total solution time in the columns “Subp. Sol. Time (s)” and “Total Sol. Time (s)” respectively, and finally the optimality gap (%). Values “TL” in the table refer to the cases that terminated because of the time limit. We consider networks with 100, 200, and 300 nodes.

Table 3 summarizes the performance of the algorithms. The average solution times are 327.6, 288.7, 233.9, 1622.0, and 116.2 seconds for the CPLEX, BD-multi, BD-multi-Pareto, BD-single, and BD-single-Pareto, respectively. The table shows that all the algorithms but the BD-single are

computationally more efficient than CPLEX, with the BD-single-Pareto being the most efficient. This is expected due to the fact that Pareto-optimal cuts are stronger and adding them as single cuts reduces their number significantly compared to multiple cuts. The BD-single algorithm is the least efficient, as shown in Table 2, it fails to solve several instances optimally within a one hour time-limit. BD-multi and BD-multi-Pareto add on average 95365.3 and 49849.3 cuts, respectively as shown in Table 3, a reduction in the number of added cuts of almost half (47%). This shows the importance and efficacy of Pareto-optimal cuts. The average number of iterations required is 18.8, 17.4, 1987.0, and 56.8 for BD-multi, BD-multi-Pareto, BD-single, BD-single-Pareto, respectively. Both multi-cut algorithms require fewer iterations to solve the instances. BD-multi-Pareto and BD-single-Pareto perform the best out of all the algorithms with BD method, therefore, we present the performance of the two algorithms and CPLEX on larger instances to test their limits. Table 4 contains the results.

We considered increasing network sizes from 400 nodes to 1000 nodes with increments of a 100, and the number of facility locations  $m$  similar to instances in Table 2. Table 4 also contains the same parameters as Table 2. Values “TL” and “Memory” refer to the termination of the algorithm because of time and memory limits, respectively. The results show that the CPLEX algorithm is unable to solve the majority of instances to proven optimality within a one-hour time limit, meanwhile the BD-multi-Pareto fails due to memory limits. The BD-single-Pareto is able to solve all instances to optimality but 4 instances, those with  $n \in \{900, 1000\}$  and  $m \in \{75, 100\}$ . BD-single-Pareto algorithm is the most efficient, it adds fewer cuts and requires the lowest number of iterations.



Table 2: Performance comparison of the BD algorithms and CPLEX on small instances.

Instance			CPLEX		BD-multi					BD-multi-Pareto					BD-single					BD-single-Pareto				
n	m	Opt. Sol. ( $10^6$ )	Total Sol. Time(s)	Gap (%)	# Iterations	# Cuts	Subp. Sol. Time (s)	Total Sol. Time (s)	Gap (%)	# Iterations	# Cuts	Subp. Sol. Time (s)	Total Sol. Time (s)	Gap (%)	# Iterations	# Cuts	Subp. Sol. Time (s)	Total Sol. Time (s)	Gap (%)	# Iterations	# Cuts	Subp. Sol. Time (s)	Total Sol. Time (s)	Gap (%)
100	5	3.17	4.4	0.0	8	19991	7.0	11.5	0.0	14	10105	11.1	15.2	0.0	6	4	1.3	1.3	0.0	10	3	1.3	2.3	0.0
	10	3.29	7.7	0.0	16	20253	7.0	13.8	0.0	16	10632	12.3	16.9	0.0	23	20	5.4	5.5	0.0	24	8	3.2	5.5	0.0
	15	3.39	10.6	0.0	36	21123	7.5	20.7	0.0	26	11430	18.3	25.0	0.0	121	115	29.9	30.2	0.0	56	22	8.1	13.4	0.0
	20	3.47	12.3	0.0	26	21341	7.7	18.4	0.0	28	11948	19.5	27.0	0.0	1440	1435	372.4	391.7	0.0	60	23	8.8	14.4	0.0
	30	3.60	11.1	0.0	16	22021	7.9	16.3	0.0	18	12706	14.2	19.5	0.0	8712	8702	2496.5	3007.5	0.0	114	45	16.6	27.3	0.0
	40	3.68	8.8	0.0	18	22719	8.1	16.1	0.0	18	12884	14.3	19.7	0.0	9440	9432	2612.7	3103.8	0.0	64	24	9.2	15.2	0.0
	50	3.74	5.5	0.0	22	22200	8.0	17.8	0.0	18	12631	14.3	19.6	0.0	8637	8632	2315.6	2942.8	0.0	46	15	6.3	10.5	0.0
	75	3.83	3.0	0.0	16	20439	7.3	14.3	0.0	10	10081	8.9	12.1	0.0	9335	9327	2528.6	3102.3	0.0	16	6	2.3	3.8	0.0
	100	3.87	0.8	0.0	6	19800	7.4	10.4	0.0	4	9900	5.8	7.4	0.0	3	2	0.6	0.6	0.0	6	2	0.8	1.4	0.0
200	5	12.35	65.5	0.0	8	79629	57.0	124.0	0.0	8	39921	59.8	84.0	0.0	4	3	6.7	6.7	0.0	10	4	9.4	14.8	0.0
	10	12.60	95.9	0.0	10	79906	57.4	130.5	0.0	12	40417	76.8	111.0	0.0	14	10	22.6	22.7	0.0	16	6	14.6	23.2	0.0
	15	12.83	116.7	0.0	22	80250	57.2	164.5	0.0	18	41003	101.9	151.1	0.0	33	29	60.1	60.3	0.0	24	9	21.6	34.5	0.0
	20	13.04	161.2	0.0	12	80567	57.6	137.6	0.0	12	41441	77.9	112.6	0.0	159	149	302.5	303.4	0.0	38	15	35.2	55.7	0.0
	30	13.42	190.0	0.0	24	81847	58.7	172.5	0.0	18	43444	103.3	151.3	0.0	520	513	1017.2	1024.5	0.0	62	20	52.5	86.0	0.0
	40	13.74	223.2	0.0	20	82848	59.2	165.6	0.0	20	44988	113.2	165.9	0.0	1815	1801	3564.3	TL	0.20	134	58	129.3	202.0	0.0
	50	14.01	207.1	0.0	34	84024	59.9	208.3	0.0	24	46059	130.0	192.2	0.0	1810	1802	3568.5	TL	0.38	152	62	141.1	223.6	0.0
	75	14.56	230.9	0.0	42	86130	61.2	234.6	0.0	34	49124	173.2	260.6	0.0	1803	1796	3567.1	TL	0.69	264	116	254.8	397.5	0.0
	100	14.94	266.9	0.0	22	86498	61.6	184.3	0.0	20	49673	116.0	170.2	0.0	1808	1799	3560.3	TL	0.93	88	34	83.1	130.3	0.0
300	5	27.69	337.0	0.0	6	179400	214.6	514.1	0.0	6	89741	187.4	265.8	0.0	4	2	15.7	15.8	0.0	8	3	27.6	43.0	0.0
	10	28.13	477.3	0.0	10	179514	214.6	568.7	0.0	8	89842	213.8	310.9	0.0	14	4	29.2	29.3	0.0	14	6	51.0	77.9	0.0
	15	28.53	621.7	0.0	10	179612	214.9	568.9	0.0	10	90232	241.2	358.8	0.0	33	4	31.3	31.4	0.0	12	5	43.6	66.8	0.0
	20	28.88	739.2	0.0	18	179958	214.9	675.6	0.0	18	91017	348.6	546.9	0.0	159	23	162.7	162.9	0.0	20	7	70.4	108.7	0.0
	30	29.50	1043.7	0.0	16	181236	215.4	653.0	0.0	20	92287	378.4	596.9	0.0	520	119	799.8	800.9	0.0	26	9	89.9	139.8	0.0
	40	30.03	1171.6	0.0	22	182898	219.7	754.6	0.0	22	94612	408.1	650.6	0.0	1815	543	3595.8	TL	0.10	54	20	182.3	286.2	0.0
	50	30.52	987.6	0.0	18	183176	219.6	709.1	0.0	20	95579	380.1	602.4	0.0	1810	545	3597.6	TL	0.22	46	16	152.5	240.8	0.0
	75	31.53	1003.5	0.0	28	187311	225.4	882.5	0.0	26	100699	468.2	760.0	0.0	1803	461	3041.6	TL	0.40	88	33	298.9	468.5	0.0
	100	32.33	840.9	0.0	22	190171	227.8	806.2	0.0	22	103535	419.0	663.9	0.0	1808	542	3595.7	TL	0.48	82	33	287.5	445.4	0.0

Table 3: Summary of computational results on small instances.

Parameter	CPLEX	BD-multi	BD-multi-Pareto	BD-single	BD-single-Pareto
Avg. # Iterations	–	18.8	17.4	1987.0	56.8
Avg. # Cuts	–	95365.3	49849.3	1770.9	22.4
Avg. Subp. Sol. Time (s)	–	94.9	152.4	1505.3	74.2
Avg. Total Sol. Time (s)	327.6	288.7	233.9	1622.0	116.2

Table 4: Performance comparison on large instances.

Problem			CPLEX		BD-multi-Pareto					BD-single-Pareto				
n	m	Opt. Sol. ( $10^6$ )	Total Sol. Time (s)	Gap (%)	# Iterations	# Cuts	Subp. Sol. Time (s)	Total Sol. Time (s)	Gap (%)	# Iterations	# Cuts	Subp. Sol. Time (s)	Total Sol. Time (s)	Gap (%)
400	5	49.12	949.7	0.0	6	159647	450.6	746.0	0.0	6	2	50.0	78.7	0.0
	10	49.70	1138.9	0.0	8	160046	520.6	899.9	0.0	8	3	70.1	108.6	0.0
	15	50.18	1649.7	0.0	12	160387	646.3	1197.0	0.0	10	4	90.6	139.4	0.0
	20	50.63	1990.3	0.0	10	160977	583.2	1044.1	0.0	10	4	100.6	148.4	0.0
	30	51.42	3088.5	0.0	20	162994	917.8	1818.8	0.0	30	11	257.5	401.5	0.0
	40	52.15	3015.3	0.0	22	164351	976.2	1948.7	0.0	34	12	285.4	448.3	0.0
	50	52.83	TL	N/A*	24	166024	1036.9	2109.6	0.0	52	18	433.9	685.0	0.0
	75	54.32	3203.5	0.0	16	169745	796.2	1526.0	0.0	40	14	335.2	526.6	0.0
	100	55.55	2942.1	0.0	28	174626	1181.6	2448.0	0.0	120	48	1086.5	1659.1	0.0
500	5	76.58	2018.0	0.0			Memory		N/A <sup>†</sup>	6	2	98.3	154.2	0.0
	10	77.39	3156.3	0.0			Memory		N/A <sup>†</sup>	6	2	100.2	156.8	0.0
	15	78.08	TL	N/A*			Memory		N/A <sup>†</sup>	10	4	178.2	272.2	0.0
	20	78.68	TL	N/A*			Memory		N/A <sup>†</sup>	16	6	279.6	431.2	0.0
	30	79.75	TL	N/A*			Memory		N/A <sup>†</sup>	28	9	449.7	714.2	0.0
	40	80.70	TL	N/A*			Memory		N/A <sup>†</sup>	32	11	545.2	847.8	0.0
	50	81.56	TL	N/A*			Memory		N/A <sup>†</sup>	22	8	393.1	601.2	0.0
	75	83.42	TL	N/A*			Memory		N/A <sup>†</sup>	36	12	611.1	949.9	0.0
	100	85.02	TL	N/A*			Memory		N/A <sup>†</sup>	32	12	553.8	858.0	0.0
600	5	110.09	TL	N/A*			Memory		N/A <sup>†</sup>	6	2	173.8	272.5	0.0
	10	110.96	TL	N/A*			Memory		N/A <sup>†</sup>	6	2	173.6	272.0	0.0
	15	111.74	TL	N/A*			Memory		N/A <sup>†</sup>	10	4	311.2	475.6	0.0
	20	112.45	TL	N/A*			Memory		N/A <sup>†</sup>	12	5	419.2	615.0	0.0
	30	113.74	TL	N/A*			Memory		N/A <sup>†</sup>	16	6	482.8	745.8	0.0
	40	114.92	TL	N/A*			Memory		N/A <sup>†</sup>	14	5	414.5	644.7	0.0
	50	116.00	TL	N/A*			Memory		N/A <sup>†</sup>	18	6	513.1	807.9	0.0
	75	118.33	TL	N/A*			Memory		N/A <sup>†</sup>	30	10	857.2	1351.0	0.0
	100	120.38	TL	N/A*			Memory		N/A <sup>†</sup>	36	12	1023.0	1615.7	0.0
	5	149.69	TL	N/A*			Memory		N/A <sup>†</sup>	6	2	280.9	440.7	0.0
	10	150.75	TL	N/A*			Memory		N/A <sup>†</sup>	6	2	280.6	438.9	0.0
	15	151.64	TL	N/A*			Memory		N/A <sup>†</sup>	8	3	392.6	603.6	0.0
	20	152.45	TL	N/A*			Memory		N/A <sup>†</sup>	10	4	502.2	764.7	0.0

\* The gap is not available because the root node relaxation cannot be solved.

† The gap is not available because of the memory limit.

(Continued on next page)

Table 4 – Performance comparison on large instances (continued)

Problem			CPLEX		Pareto multi-cut					Pareto single-cut				
n	m	Opt. Sol. ( $10^6$ )	Total Sol. Time (s)	Gap (%)	# Iterations	# Cuts	Subp. Sol. Time (s)	Total Sol. Time (s)	Gap (%)	# Iterations	# Cuts	Subp. Sol. Time (s)	Total Sol. Time (s)	Gap (%)
700	30	153.95	TL	N/A*			Memory		N/A <sup>†</sup>	12	5	612.0	928.6	0.0
	40	155.34	TL	N/A*			Memory		N/A <sup>†</sup>	14	5	667.2	1037.8	0.0
	50	156.60	TL	N/A*			Memory		N/A <sup>†</sup>	16	7	900.8	1327.5	0.0
	75	159.42	TL	N/A*			Memory		N/A <sup>†</sup>	28	10	1338.8	2086.8	0.0
	100	161.95	TL	N/A*			Memory		N/A <sup>†</sup>	30	9	1319.6	2116.3	0.0
800	5	195.35	TL	N/A*			Memory		N/A <sup>†</sup>	6	2	433.5	677.4	0.0
	10	196.56	TL	N/A*			Memory		N/A <sup>†</sup>	6	2	436.4	681.9	0.0
	15	197.63	TL	N/A*			Memory		N/A <sup>†</sup>	6	2	434.5	678.4	0.0
	20	198.61	TL	N/A*			Memory		N/A <sup>†</sup>	14	6	1124.1	1693.4	0.0
	30	200.40	TL	N/A*			Memory		N/A <sup>†</sup>	10	4	781.6	1194.7	0.0
	40	202.02	TL	N/A*			Memory		N/A <sup>†</sup>	18	8	1572.9	2309.9	0.0
	50	203.43	TL	N/A*			Memory		N/A <sup>†</sup>	16	6	1228.4	1895.0	0.0
	75	206.63	TL	N/A*			Memory		N/A <sup>†</sup>	28	9	2080.5	3247.3	0.0
100	209.48	TL	N/A*			Memory		N/A <sup>†</sup>	14	6	1132.8	1715.8	0.0	
900	5	246.65	TL	N/A*			Memory		N/A <sup>†</sup>	6	2	620.8	967.3	0.0
	10	247.91	TL	N/A*			Memory		N/A <sup>†</sup>	8	3	879.4	1348.5	0.0
	15	249.03	TL	N/A*			Memory		N/A <sup>†</sup>	8	3	870.1	1335.1	0.0
	20	250.10	TL	N/A*			Memory		N/A <sup>†</sup>	12	5	1366.3	2082.8	0.0
	30	252.08	TL	N/A*			Memory		N/A <sup>†</sup>	10	4	1118.0	1709.4	0.0
	40	253.92	TL	N/A*			Memory		N/A <sup>†</sup>	10	4	1117.8	1713.4	0.0
	50	255.65	TL	N/A*			Memory		N/A <sup>†</sup>	8	3	871.2	1342.8	0.0
	75	259.42	TL	N/A*			Memory		N/A <sup>†</sup>	22	8	TL	TL	0.01
	100	262.84	TL	N/A*			Memory		N/A <sup>†</sup>	20	7	TL	TL	0.01
1000	5	304.36	TL	N/A*			Memory		N/A <sup>†</sup>	6	2	888.7	1387.7	0.0
	10	305.75	TL	N/A*			Memory		N/A <sup>†</sup>	6	2	884.5	1388.2	0.0
	15	307.04	TL	N/A*			Memory		N/A <sup>†</sup>	8	3	1239.6	1915.0	0.0
	20	308.22	TL	N/A*			Memory		N/A <sup>†</sup>	10	4	1614.8	2463.6	0.0
	30	310.41	TL	N/A*			Memory		N/A <sup>†</sup>	10	4	1597.6	2460.0	0.0
	40	312.44	TL	N/A*			Memory		N/A <sup>†</sup>	10	4	1582.8	2420.0	0.0
	50	314.31	TL	N/A*			Memory		N/A <sup>†</sup>	16	7	2648.1	3451.6	0.0
	75	318.57	TL	N/A*			Memory		N/A <sup>†</sup>	28	10	TL	TL	0.01
100	322.38	TL	N/A*			Memory		N/A <sup>†</sup>	24	9	TL	TL	0.01	

\* The gap is not available because the root node relaxation cannot be solved.

<sup>†</sup> The gap is not available because of the memory limit.

## 5. Chicago Case Study

In this section, we present the results of a case study on a real-world Chicago network. We use publicly available census data from 2010 for population counts, commuting patterns using personal vehicles and OD pair information (Dash Nelson and Rae, 2016), and data from Chicago Transit

Table 5: Chicago dataset characteristics.

Population (million)	# Nodes	# OD pairs	Node Density (#/km <sup>2</sup> )	Distance (km)	
				minimum	maximum
2.701	797	35501	1.353	0.19	62.1

Authority for public transportation commuting counts (City of Chicago, 2020). The network representing this dataset is shown in Figure 2 and its characteristics are summarized in Table 5. The network contains 2.701 million customers aggregated into 797 nodes, 35501 OD pairs with a node density of 1.353 nodes/km<sup>2</sup>. The minimum and maximum direct distance between a pair of nodes is 0.19 and 52.1 km, respectively. We consider coverage distance  $d \in \{1, 2, 3\}$ . We use Manhattan distance due to the grid structure of the road network of the city of Chicago. We consider driving deviation tolerances  $\lambda \in \{10\%, 30\%, 50\%\}$ . Availability time, maximum availability time and numbers of potential locations are selected similar to the random dataset. We consider personal vehicle commuting counts, representing 34% of the total customer demand, as the demand that can be captured on OD pairs or at origin and destination, the public transportation counts, representing 45% of the total demand, as the demand that can be captured at the origin and destination, and the rest 21% of the population count as demand that can only covered at the origin (Dash Nelson and Rae, 2016).

### 5.1. Computational Performance

We use BD-single-Pareto implementation as the solution method and present the computational efficiency on solving the problem instances of the Chicago case study. Table 6 presents the computational results on instances with varying number of facility locations  $m$  and coverage distances  $d$ . The driver tolerance  $\lambda$  has an insignificant impact on the performance of the algorithm. Therefore, we report the average performance of  $\lambda \in \{10\%, 30\%, 50\%\}$  in Table 6. The two left-most columns show the coverage distance  $d$  and the number of facilities  $m$ , columns 3–6 display the number of subproblems, the number of cuts added, the total subproblem solution time and the total solution time. Although the total solution time increases significantly for larger  $d$  and  $m$  values, the BD-single-Pareto implementation solves all the instances within the one-hour time limit.

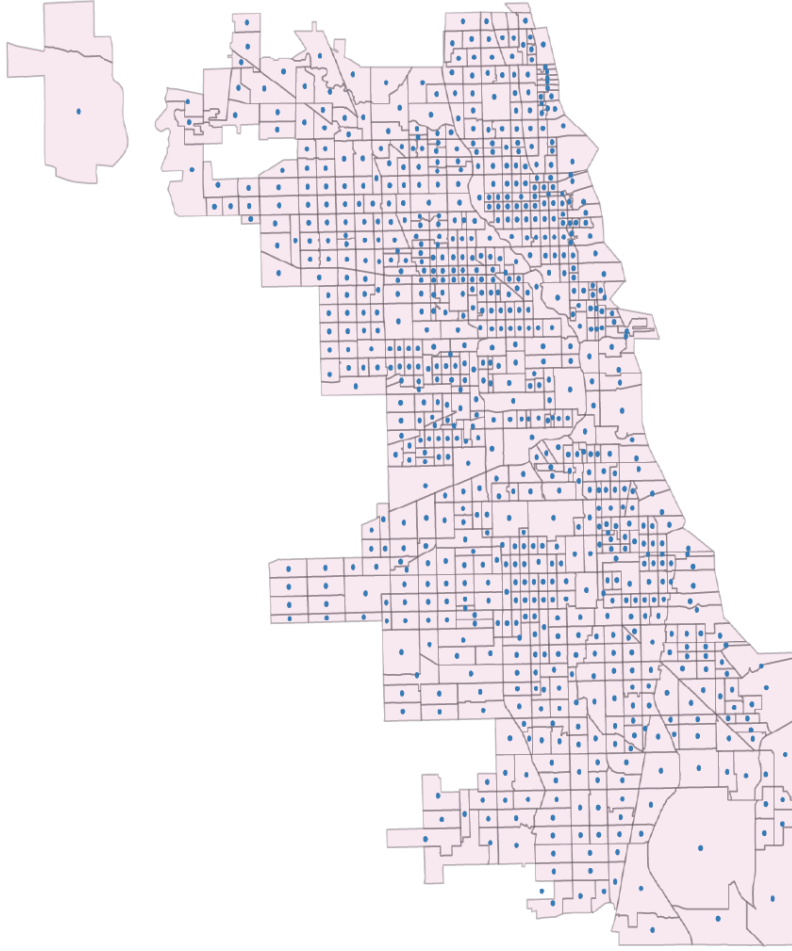


Figure 2: Chicago network and 797 nodes representing the census tracts (City of Chicago, 2018).

## 5.2. Discussion

In this section, we present the results of the Chicago dataset, compare the impacts of different settings on the demand coverage. We first investigate the change in coverage with the number of facilities  $m$ . Figure 3 represents the percentage of coverage for increasing number of facilities in the city of Chicago. Each red dot represents an open facility and the highlighted areas on the maps represent the areas covered. Areas that are highlighted but do not include any facilities at their center are areas housing customers that can be covered along their OD paths. As can be seen from the figure, increasing the number of facilities, expands the coverage significantly. We can only cover 32.08% with 20 facilities but more than 75% with 80 open facilities. Figures 4 (a) and (b) confirm the findings that the demand coverage increases with greater number of facilities  $m$  regardless of the coverage distance  $d$  and driving tolerance  $\lambda$ . Figure 4(a) also shows that we

Table 6: Performance of BD-single-Pareto on Chicago dataset.

d	m	# Subproblems	# Cuts	Subp. Sol. Time (s)	Total Sol. Time (s)
1	10	40	14	5.9	12.0
	20	116	48	18.9	36.2
	40	324	188	68.1	119.4
	60	774	336	114.8	347.2
	80	1796	874	319.7	1372.2
	100	2442	1196	438.2	2944.2
3	10	46	18	7.3	14.2
	20	121	52	22.8	56.5
	40	386	212	86.4	185.6
	60	806	362	128.6	393.9
	80	1944	928	362.1	1716.9
	100	2662	1232	473.8	3103.6
5	10	78	32	15.3	34.0
	20	278	208	78.5	155.9
	40	604	296	178.3	795.4
	60	1216	572	285.6	1003.5
	80	2087	1003	402.9	2093.0
	100	2940	1445	512.8	3520.0

are able to cover 93% of the demand with 40 facilities when  $d = 3$  but only 49% with the same number of facilities with  $d = 1$ . We can also cover nearly the same percentage of the population with 20 facilities with  $d = 3$  (73%) as 80 facilities with  $d = 1$  (75%). These results prove that the coverage distance  $d$  has a bigger impact on the percentage of demand served compared to the number of facilities  $m$ , and increasing the coverage distance of facilities allows us to cover more customer demand compared to increasing the number of facilities  $m$ . The coverage distance also affects where we capture the demand, as can be seen from Figure 5(a). Increasing the value of  $d$  means that we are able to cover more demand around origin and destination nodes rather than on OD paths.

We have also tested the impact of the driver tolerance  $\lambda$  on the demand coverage. Figure 4(b)

shows that increasing the driving tolerance positively impacts the percentage of covered demand. Nevertheless, the increase is not as significant as the one induced by larger coverage distances. On average the number of facilities decreases by 20 from  $\lambda = 0\%$  to  $\lambda = 50\%$  for the same percentage of coverage, while the number of facilities decreases by 60 from  $d = 1$  to  $d = 5$ . The driving tolerance impacts where the demand is captured. Figure 5(b) shows that for the instance with  $d = 1$  and  $m = 60$ , the higher the value of  $\lambda$  the more demand is captured on paths. The driver tolerance can have more impact in less dense and more sparse areas where personal vehicles are more widely used.

An important application of the model presented is the location of testing facilities during a pandemic as discussed in Section 1. In the following, we present the impact of a confinement during a pandemic on the demand coverage. To simulate a pandemic situation, we create three different datasets from the Chicago dataset. We use public transportation total counts during the period of April 2020, June 2020, and July 2020 as a representation of the drop in commuting counts during the different stages of the pandemic and project them on the rest of the data. The 3 months represent three different levels of confinement: high, moderate, and low, and each level is associated with a confinement percentage representing the decrease in travel. The high level represents an 80% decrease in travel, the moderate level a 60% decrease and the low level a 40% decrease. We refer to the levels as level 0 for no travel restrictions, and level 1, 2, and 3 for the low, moderate and high confinement stages, respectively.

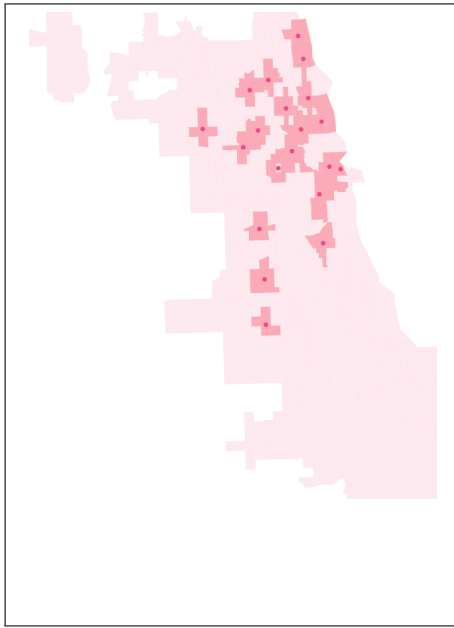
Figure 4(c) shows that the percentage of coverage is not affected by a confinement situation, we can still cover approximately the same percentage of the population regardless of the travel restrictions. The way in which the demand is captured changes drastically, Figure 5(c) shows that higher levels of confinement signify capturing more demand around origins rather than around destinations or on OD paths. This result is in accordance with a real-life pandemic situation, as less people are able to travel and work from home is more prevalent. We also investigate the effects of existing facility set-ups on coverage. We measure the percentage of coverage change of a facility set-up optimized for level  $u$  compared to a facility set-up optimized for level  $v$ , we refer to this change as the cost of immobility (CI).  $CI(u, v)$  represents the loss of coverage of a set-up optimized using data from level  $u$  applied to data from level  $v$ . For instance, the facility set-up illustrated in Figure 3(a) optimized with data from level 0, applied to data from level 3 induces an 8.1% loss in

coverage. To define  $CI(u, v)$ , let  $z_v(u)$  the objective function value of the optimal solution of level  $v$  evaluated using the demand data from level  $u$ . The cost of immobility is then defined as follows:

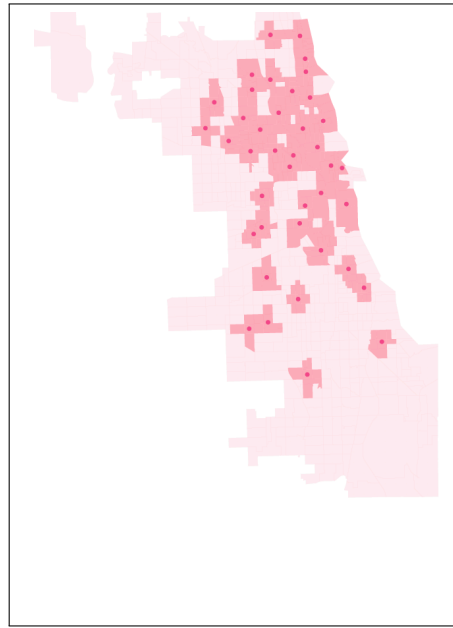
$$CI(u, v) = \frac{z_v(u) - z_u(u)}{z_v(v)}.$$

Figures 6 present the cost of immobility matrices for all levels of confinement and different number of facilities. Each matrix entry contains the cost of immobility induced by the transition from the optimization level to the current level. For instance, a set-up with 20 facilities optimized with data from level 0 costs up to 8% in coverage when level 3 travel restrictions come into effect. As can be seen from Figure 6, the cost of immobility from level 0 to 3 ( $CI(0,3)$ ) is higher than the cost of immobility from level 3 to level 0 ( $CI(3,0)$ ) ( $8.1 > 4.2$ ). For  $m = 20$ , on average, the cost of immobility when phasing out confinement is 2.46%, while the cost of immobility when entering confinement is 4.55%. Similar findings are true for different  $m$  values. This signifies that the optimization is more effective when confinement and travel restriction data is taken into account. Figures 6 also show that the cost of immobility decreases with a higher number of facilities. For example,  $CI(0,3) = -8.1\%$  with  $m = 20$  but only  $-2.3\%$  with  $m = 80$ . The experiments mark the importance of mobile facilities for providing testing services during such rapidly changing environments as pandemics. Indeed, buses were converted into mobile testing facilities in Montreal during the Covid-19 pandemic (Lalonde, 2020).

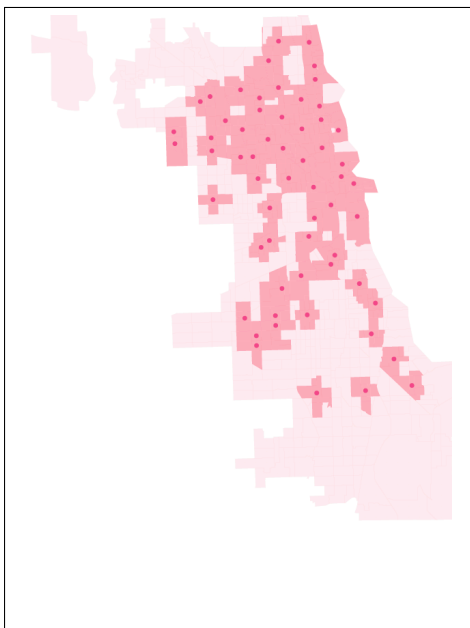




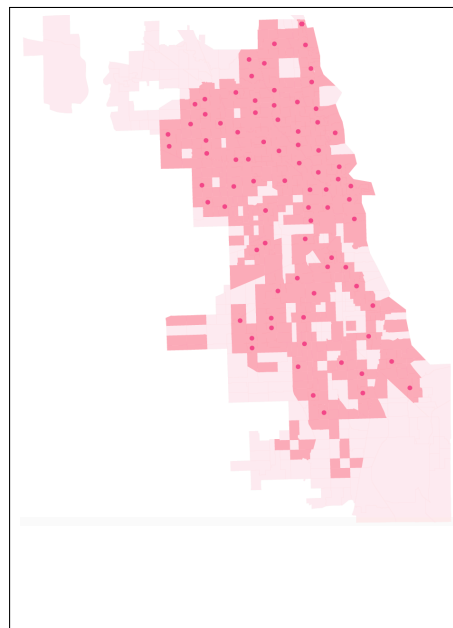
(a) Facilities = 20, Coverage = 32.08%



(b) Facilities = 40, Coverage = 49.70%

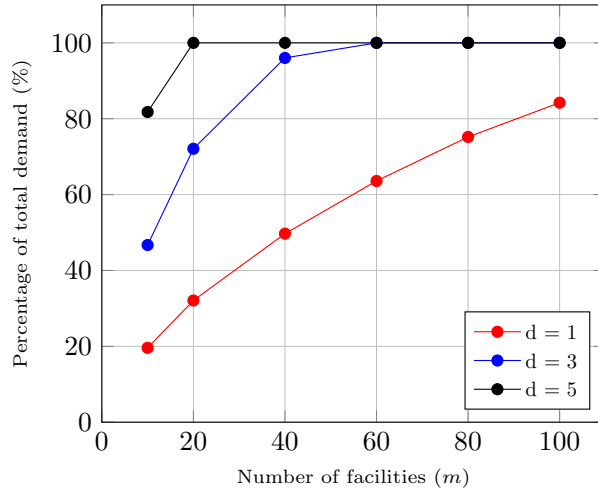


(c) Facilities = 60, Coverage = 63.59%

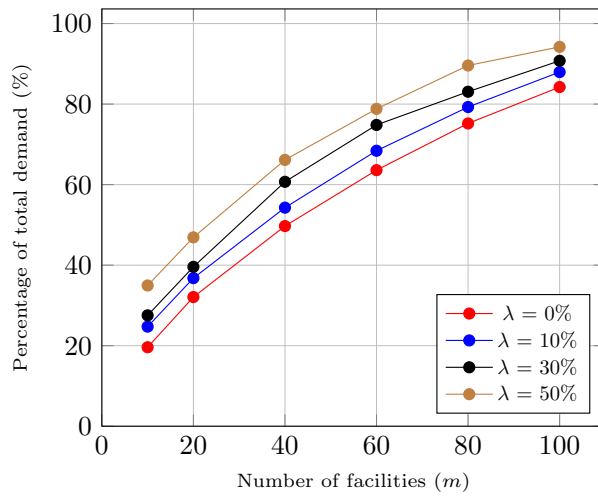


(d) Facilities = 80, Coverage = 75.19%

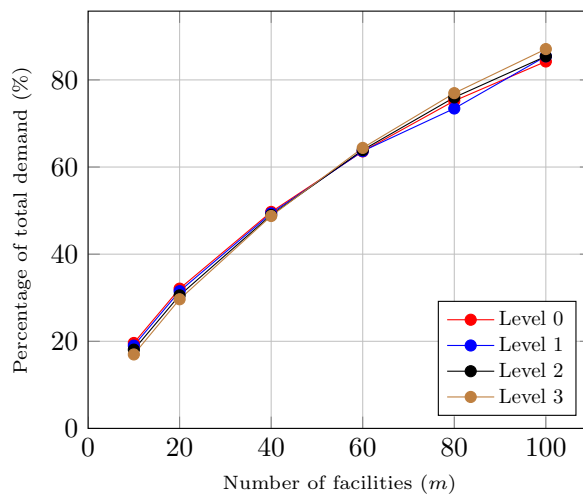
Figure 3: Facility locations and their coverage for Chicago network for level 0,  $d = 1$  and  $\lambda = 0\%$  with  $m \in \{20, 40, 60, 100\}$  in figures (a), (b), (c), and (d), respectively.



(a) Percentage of total demand covered for Level 0 and  $\lambda = 0$

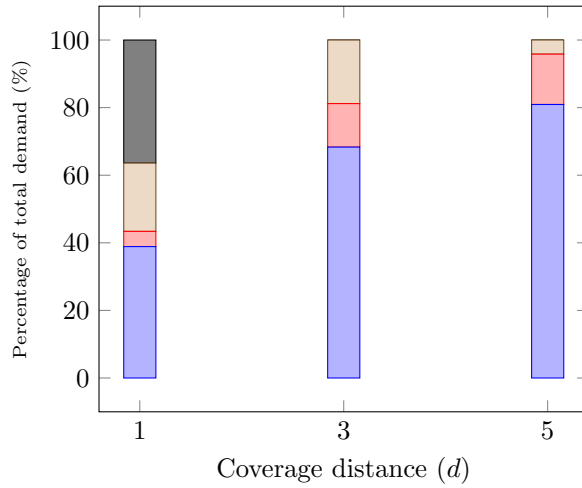


(b) Percentage of total demand covered for Level 0 and  $d = 1$

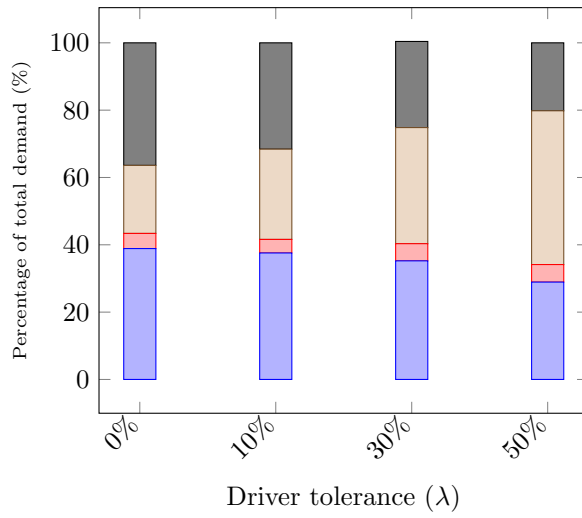


(c) Percentage of total demand covered for  $\lambda = 0\%$  and  $d = 1$

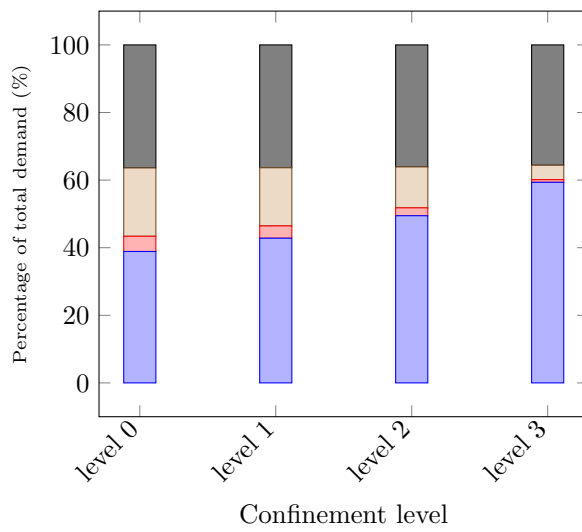
Figure 4: Percentage of demand coverage with  $m \in \{10, 20, 40, 60, 80, 100\}$  for different  $d$ ,  $\lambda$ , and confinement level in figures (a), (b), and (c), respectively.



(a) Type of coverage for  $m = 60$ , Level 0, and  $\lambda = 0\%$



(b) Type of coverage for  $m = 60$ , Level 0, and  $d = 1$



(c) Type of coverage for  $m = 60$ ,  $\lambda = 0\%$ , and  $d = 1$

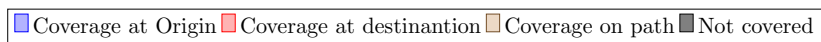


Figure 5: Type of coverage for varying  $d$ ,  $\lambda$ , and confinement level in figures (a), (b), and (c), respectively.

		Current Level			
		0	1	2	3
Optimization level	0	0	-3.1	-5.7	-8.1
	1	-1.7	0	-2.9	-4.8
	2	-2.8	-2.1	0	-2.7
	3	-4.2	-2.9	-1.1	0

(a) CI (%) with  $m = 20$

		Current Level			
		0	1	2	3
Optimization level	0	0	-2.3	-4.1	-6.9
	1	-1.1	0	-2.0	-3.9
	2	-2.1	-1.7	0	-1.5
	3	-3.8	-1.9	-0.9	0

(b) CI (%) with  $m = 40$

		Current Level			
		0	1	2	3
Optimization level	0	0	-1.3	-2.7	-4.1
	1	-0.8	0	-1.4	-3.1
	2	-1.7	-1.2	0	-1.1
	3	-3.0	-1.2	-0.6	0

(c) CI (%) with  $m = 60$

		Current Level			
		0	1	2	3
Optimization level	0	0	-1.0	-2.1	-2.9
	1	-0.5	0	-1.0	-1.7
	2	-1.1	-0.8	0	-1.1
	3	-2.3	-0.8	-0.3	0

(d) CI (%) with  $m = 80$

Figure 6: Cost of immobility (CI) for all levels of confinement with  $m = 20, 40, 60, 80$  facilities, in figures (a), (b), (c), (d), respectively.

## 6. Conclusion

We have presented the maximum availability service facility location problem, in which facility locations are optimized by taking into account the stationary and mobile demand in an urban region. Stationary customers are covered at their origins, the population using the public transportation are covered at their origins or destinations, and personal vehicle users are covered at their origins, destinations or on their commute paths. This problem has applications in location of government offices, medical facilities for testing and vaccination purposes, or polling stations. We have presented a MILP formulation to the problem and have developed a Benders decomposition algorithm. We have proposed an analytical solution to the BD subproblems as well as four different cut implementations to solve problem instances: single-cut, multi-cut, Pareto-optimal single-cut and Pareto-optimal multi-cut. We have conducted extensive experiments and showed on randomly generated datasets that the Pareto-optimal single-cut implementation performs better than all other BD implementations and better than CPLEX. CPLEX is unable to solve large instances within a one hour time limit and the Pareto multiple cut implementation struggles due to memory limits. In addition, we have conducted a case study on the city of Chicago and simulated a confinement situation during a pandemic. We have found that with our model, we are capable of capturing the similar demand volumes for all levels of confinement and that locating facilities is more efficient when travel restrictions are taken into account during the optimization.

For future research directions, facility capacities, resource constraints, and a time dimension can be added to the model to make the problem more realistic. Adding uncertainty for the travel flows and demand would make the problem more applicable in the real-world. A robust optimization approach can also help in providing a minimum level of coverage during different phases of confinement for fixed facilities.

## References

- Arslan, O., Jabali, O., Laporte, G., 2018. Exact solution of the evasive flow capturing problem. *Operations Research* 66, 1625–1640.
- Arslan, O., Karaşan, O.E., 2016. A Benders decomposition approach for the charging station location problem with plug-in hybrid electric vehicles. *Transportation Research Part B: Methodological* 93, 670–695.
- Benders, J.F., 1962. Partitioning procedures for solving mixed-variables programming problems. *Numerische Mathematik* 4, 238–252.
- Berman, O., Bertsimas, D., Larson, R.C., 1995. Locating discretionary service facilities, II: Maximizing market size, minimizing inconvenience. *Operations Research* 43, 623–632.
- Berman, O., Larson, R., Fouska, N., 1992. Optimal location of discretionary service facilities. *Transportation Science* 26, 161–260.
- Chauhan, D., Unnikrishnan, A., Figliozzi, M., 2019. Maximum coverage capacitated facility location problem with range constrained drones. *Transportation Research Part C: Emerging Technologies* 99, 1–18.
- City of Chicago, 2018. Boundaries - census tracts - 2010. URL: <https://data.cityofchicago.org/Facilities-Geographic-Boundaries/Boundaries-Census-Tracts-2010/5jrd-6zik>. accessed: 2020-08-30.
- City of Chicago, 2020. CTA - ridership - 'L' station entries - daily totals. URL: <https://data.cityofchicago.org/Transportation/CTA-Ridership-L-Station-Entries-Daily-Totals/5neh-572f>. accessed: 2020-08-30.
- Codato, G., Fischetti, M., 2006. Combinatorial Benders cuts for mixed-integer linear programming. *Operations Research* 54, 756–766.
- Cordeau, J.-F., Furini, F., Ljubić, I., 2019. Benders decomposition for very large scale partial set covering and maximal covering location problems. *European Journal of Operational Research* 275, 882–896.
- Costa, A.M., 2005. A survey on Benders decomposition applied to fixed-charge network design problems. *Computers & Operations Research* 32, 1429–1450.
- Dash Nelson, G., Rae, A., 2016. An economic geography of the United States: From commutes to megaregions. *PLOS ONE* 11, 1–23.
- de Camargo, R., Miranda, G., Luna, H., 2008. Benders decomposition for the uncapacitated multiple allocation hub location problem. *Computers & Operations Research* 35, 1047–1064.
- Erkut, E., Ingolfsson, A., Erdoğan, G., 2008. Ambulance location for maximum survival. *Naval Research Logistics* 55, 42–58.
- García, S., Marín, A., 2019. Covering location problems, in: Laporte, G., Nickel, S., Saldanha da Gama, F. (Eds.), *Location Science*. Springer. chapter 5, pp. 99–119.
- Hodgson, M.J., 1990. A flow-capturing location-allocation model. *Geographical Analysis* 22, 270–279.
- Hodgson, M.J., Rosing, K.E., Leontien, A., Storrier, G., 1996. Applying the flow-capturing location-allocation model to an authentic network: Edmonton, Canada. *European Journal of Operational Research* 90, 427–443.
- Kim, J.G., Kuby, M., 2012. The deviation-flow refueling location model for optimizing a network of refueling stations. *International Journal of Hydrogen Energy* 37, 5406–5420.
- Kuby, M., Lim, S., 2005. The flow-refueling location problem for alternative-fuel vehicles. *Socio-Economic Planning Sciences* 39, 125–145.
- Lalonde, M., 2020. Montreal city buses to be used as mobile testing clinics. URL: <https://montrealgazette.com/news/montreal-reports-78-new-covid-19-deaths-385-new-cases>. accessed: 2020-08-30.
- Magnanti, T.L., Wong, R.T., 1981. Accelerating Benders decomposition: Algorithmic enhancement and model selection criteria. *Operations Research* 29, 464–484.
- Marković, N., Ryzhov, I.O., Schonfeld, P., 2015. Evasive flow capture: Optimal location of weigh-in-motion systems, tollbooths, and security checkpoints. *Networks* 65, 22–42.
- Murali, P., Ordóñez, F., Dessouky, M.M., 2012. Facility location under demand uncertainty: Response to a large-scale bio-terror attack. *Socio-Economic Planning Sciences* 46, 78–87.

- Papadakos, N., 2008. Practical enhancements to the Magnanti–Wong method. *Operations Research Letters* 36, 444–449.
- Rahmaniani, R., Crainic, T.G., Gendreau, M., Rei, W., 2017. The Benders decomposition algorithm: A literature review. *European Journal of Operational Research* 259, 801–817.
- Riemann, R., Wang, D.Z., Busch, F., 2015. Optimal location of wireless charging facilities for electric vehicles: Flow-capturing location model with stochastic user equilibrium. *Transportation Research Part C: Emerging Technologies* 58, 1–12.
- Snyder, L.V., 2011. Covering problems, in: Eiselt, H.A., Marianov, V. (Eds.), *Foundations of Location Analysis*. Springer. chapter 6, pp. 109–135.
- Taymaz, S., Iyigun, C., Bayindir, Z., Dellaert, N., 2020. A healthcare facility location problem for a multi-disease, multi-service environment under risk aversion. *Socio-Economic Planning Sciences* 71, 100755.
- Turkoglu, D.C., Genevois, M.E., 2020. A comparative survey of service facility location problems. *Annals of Operations Research* 292, 399–468.
- Upchurch, C., Kuby, M., Lim, S., 2009. A model for location of capacitated alternative-fuel stations. *Geographical Analysis* 41, 85–106.
- Wen, M., Laporte, G., Madsen, O.B.G., Nørrelund, A.V., Olsen, A., 2014. Locating replenishment stations for electric vehicles: application to danish traffic data. *Journal of the Operational Research Society* 65, 1555–1561.
- Yıldız, B., Arslan, O., Karahan, O.E., 2016. A branch and price approach for routing and refueling station location model. *European Journal of Operational Research* 248, 815–826.
- You, F., Grossmann, I.E., 2013. Multicut Benders decomposition algorithm for process supply chain planning under uncertainty. *Annals of Operations Research* 210, 191–211.
- Zetina, C.A., Contreras, I., Cordeau, J.-F., 2019. Exact algorithms based on Benders decomposition for multicommodity uncapacitated fixed-charge network design. *Computers & Operations Research* 111, 311–324.

## Chapitre 3: Conclusion

Nous avons présenté le problème de “*maximum availability service facility location problem*”, dans lequel l’emplacement des établissements est optimisé en tenant compte de la demande stationnaire et mobile en milieu urbain. Les clients stationnaires sont couverts à l’origine, la population utilisant les transports publics est couverte à l’origine ou à la destination, et les utilisateurs de véhicules personnels sont couverts à l’origine, à la destination ou sur le trajet domicile-travail. Ce problème a des applications dans la localisation des bureaux gouvernementaux, des centres médicaux de dépistage et de vaccination, ou des bureaux de vote. Nous avons présenté une formulation MILP au problème et avons développé un algorithme de décomposition de Benders. Nous avons ensuite proposé une solution analytique aux sous-problèmes BD ainsi que quatre différents implémentations de coupes pour résoudre les problèmes: coupe singulière, coupe multiple, coupe Pareto-optimale singulière et coupe Pareto-optimale multiple. Nous avons mené des expériences approfondies et montré à travers des données générées aléatoirement que la coupe Pareto-optimale singulière surperforme toutes les autres implémentations BD et offre un meilleur résultat que CPLEX. Ce dernier est incapable de résoudre de grandes instances en une seule heure limite. L’implémentation coupe Pareto-optimale multiple pose des difficultés en raison des limites de la mémoire. Nous avons mené une étude de cas sur la ville de Chicago et simulé un confinement pendant une pandémie. Nous avons constaté qu’avec notre modèle, nous sommes capables de capturer des volumes de demande similaires pour tous les niveaux de confinement, et que la localisation des installations est plus efficace lorsque les restrictions de déplacement sont prises en compte lors de l’optimisation. Pour des futures orientations de recherche, les capacités des installations, les contraintes de ressources et une dimension temporelle peuvent être ajoutées au modèle pour rendre le problème plus réaliste. Ajouter



de l'incertitude aux flux des trajets et à la demande rendrait le problème plus applicable dans le monde réel. Une approche d'optimisation robuste peut également aider à fournir un niveau minimum de couverture au cours des différentes phases de confinement pour les installations fixes.

# Bibliographie

## References

- Arslan, O., Jabali, O., Laporte, G., 2018. Exact solution of the evasive flow capturing problem. *Operations Research* 66, 1625–1640.
- Arslan, O., Karaşan, O.E., 2016. A Benders decomposition approach for the charging station location problem with plug-in hybrid electric vehicles. *Transportation Research Part B: Methodological* 93, 670–695.
- Benders, J.F., 1962. Partitioning procedures for solving mixed-variables programming problems. *Numerische Mathematik* 4, 238–252.
- Berman, O., Bertsimas, D., Larson, R.C., 1995. Locating discretionary service facilities, II: Maximizing market size, minimizing inconvenience. *Operations Research* 43, 623–632.
- Berman, O., Larson, R., Fouska, N., 1992. Optimal location of discretionary service facilities. *Transportation Science* 26, 161–260.
- Chauhan, D., Unnikrishnan, A., Figliozzi, M., 2019. Maximum coverage capacitated facility location problem with range constrained drones. *Transportation Research Part C: Emerging Technologies* 99, 1–18.
- City of Chicago, 2018. Boundaries - census tracts - 2010. URL: <https://data.cityofchicago.org/Facilities-Geographic-Boundaries/Boundaries-Census-Tracts-2010/5jrd-6zik>. accessed: 2020-08-30.
- City of Chicago, 2020. CTA - ridership - 'L' station entries - daily totals. URL: <https://data.cityofchicago.org/Transportation/CTA-Ridership-L-Station-Entries-Daily-Totals/5neh-572f>. accessed: 2020-08-30.
- Codato, G., Fischetti, M., 2006. Combinatorial Benders cuts for mixed-integer linear programming. *Operations Research* 54, 756–766.
- Cordeau, J.-F., Furini, F., Ljubić, I., 2019. Benders decomposition for very large scale partial set covering and maximal covering location problems. *European Journal of Operational Research* 275, 882–896.
- Costa, A.M., 2005. A survey on Benders decomposition applied to fixed-charge network design problems. *Computers & Operations Research* 32, 1429–1450.
- Dash Nelson, G., Rae, A., 2016. An economic geography of the United States: From commutes to megaregions. *PLOS ONE* 11, 1–23.
- de Camargo, R., Miranda, G., Luna, H., 2008. Benders decomposition for the uncapacitated multiple allocation hub location problem. *Computers & Operations Research* 35, 1047–1064.
- Erkut, E., Ingolfsson, A., Erdoğan, G., 2008. Ambulance location for maximum survival. *Naval Research Logistics* 55, 42–58.
- García, S., Marín, A., 2019. Covering location problems, in: Laporte, G., Nickel, S., Saldanha da Gama, F. (Eds.), *Location Science*. Springer. chapter 5, pp. 99–119.
- Hodgson, M.J., 1990. A flow-capturing location-allocation model. *Geographical Analysis* 22, 270–279.
- Hodgson, M.J., Rosing, K.E., Leontien, A., Storrier, G., 1996. Applying the flow-capturing location-allocation model to an authentic network: Edmonton, Canada. *European Journal of Operational Research* 90, 427–443.
- Kim, J.G., Kuby, M., 2012. The deviation-flow refueling location model for optimizing a network of refueling stations. *International Journal of Hydrogen Energy* 37, 5406–5420.
- Kuby, M., Lim, S., 2005. The flow-refueling location problem for alternative-fuel vehicles. *Socio-Economic Planning Sciences* 39, 125–145.
- Lalonde, M., 2020. Montreal city buses to be used as mobile testing clinics. URL: <https://montrealgazette.com/news/montreal-reports-78-new-covid-19-deaths-385-new-cases>. accessed: 2020-08-30.
- Magnanti, T.L., Wong, R.T., 1981. Accelerating Benders decomposition: Algorithmic enhancement and model selection criteria. *Operations Research* 29, 464–484.

- Marković, N., Ryzhov, I.O., Schonfeld, P., 2015. Evasive flow capture: Optimal location of weigh-in-motion systems, tollbooths, and security checkpoints. *Networks* 65, 22–42.
- Murali, P., Ordóñez, F., Dessouky, M.M., 2012. Facility location under demand uncertainty: Response to a large-scale bio-terror attack. *Socio-Economic Planning Sciences* 46, 78–87.
- Papadakos, N., 2008. Practical enhancements to the Magnanti–Wong method. *Operations Research Letters* 36, 444–449.
- Rahmaniani, R., Crainic, T.G., Gendreau, M., Rei, W., 2017. The Benders decomposition algorithm: A literature review. *European Journal of Operational Research* 259, 801–817.
- Riemann, R., Wang, D.Z., Busch, F., 2015. Optimal location of wireless charging facilities for electric vehicles: Flow-capturing location model with stochastic user equilibrium. *Transportation Research Part C: Emerging Technologies* 58, 1–12.
- Snyder, L.V., 2011. Covering problems, in: Eiselt, H.A., Marianov, V. (Eds.), *Foundations of Location Analysis*. Springer. chapter 6, pp. 109–135.
- Taymaz, S., Iyigun, C., Bayindir, Z., Dellaert, N., 2020. A healthcare facility location problem for a multi-disease, multi-service environment under risk aversion. *Socio-Economic Planning Sciences* 71, 100755.
- Turkoglu, D.C., Genevois, M.E., 2020. A comparative survey of service facility location problems. *Annals of Operations Research* 292, 399–468.
- Upchurch, C., Kuby, M., Lim, S., 2009. A model for location of capacitated alternative-fuel stations. *Geographical Analysis* 41, 85–106.
- Wen, M., Laporte, G., Madsen, O.B.G., Nørrelund, A.V., Olsen, A., 2014. Locating replenishment stations for electric vehicles: application to danish traffic data. *Journal of the Operational Research Society* 65, 1555–1561.
- Yıldız, B., Arslan, O., Karahan, O.E., 2016. A branch and price approach for routing and refueling station location model. *European Journal of Operational Research* 248, 815–826.
- You, F., Grossmann, I.E., 2013. Multicut Benders decomposition algorithm for process supply chain planning under uncertainty. *Annals of Operations Research* 210, 191–211.
- Zetina, C.A., Contreras, I., Cordeau, J.-F., 2019. Exact algorithms based on Benders decomposition for multicommodity uncapacitated fixed-charge network design. *Computers & Operations Research* 111, 311–324.